KWAME NKRUMAH UNIVERSITY OF SCIENCE
AND TECHNOLOGY, KUMASI, GHANA

Integrating Gravity and Magnetic Field Data to Delineate Structurally-Controlled Gold Mineralization in the Sefwi Belt

By

Bernard Owuraku Kanin (Bsc. Geological Engineering)

A Thesis submitted to the Department of Geological Engineering
College of Engineering
in partial fulfillment of the requirements for the degree of

MASTER OF SCIENCE

OCTOBER, 2016

Declaration

I hereby declare that this submission is my own work towards the MSc and that, to the best of my knowledge; it contains no material previously published by another person or material which has been accepted for the award of any other degree of the University, except where due acknowledgment has been made in the text.

....	....….......……	…………
Student Name & ID	Signature	Date

Certified by:

....	....	....
Supervisor(s) Name	Signature	Date

Certified by:

....	. ...	....
Supervisor(s) Name	Signature	Date

Certified by:

....	....	……......................
Head of Dept.Name	Signature	Date

Abstract

Gravity and magnetic surveys have been used to delineate potential gold mineralization on the Sefwi belt of Ghana. The study area, which is intrusive dominated hosting pockets of small scale mining operations locally referred to as Galamsey, is without any scientific trend of gold mineralization. The study aims at mapping lithological units, structural setting and relating Galamsey sites to delineate potential zones of gold mineralization. Scintrex CG5 gravimeter and GEM's Overhauser magnetometer were used for gravity and magnetic data acquisition respectively. The magnetic data were corrected and enhancing filters such as RTP, analytical signal and 1VD were applied using oasis montaj 7.1. Gravity data were also reduced to a common datum (geoid) using the oasis montaj software to produce a Bouguer anomaly map. Regional/residual separation technique produced a residual gravity map. The RTP and analytical signal filters from the magnetic data and residual gravity anomaly map from the gravity data helped in mapping belt type (Dixcove) Birimian granitoids and mafic intrusive unit, interpreted as gabbro. The first vertical derivative filter was useful in mapping NE/SW minor faults and crosscutting dykes largely concentrated in the belt type Birimian granitoids. All the three mapped Galamsey sites fell on a minor fault and are associated with the belt type granitoids which have been a lead in delineating potential zones of gold mineralization.

Contents

List of Figures

List of symbols and acronyms

IP Induced Polarization GD

Granitoid Unit µ Magnetic

permeability

F Magnetic/Gravitational force

H Magnetic field strength B Flux density μ_r

Relative Permeability k magnetic

susceptibility μ_o Permeability of vacuum D

Angle of declination

I Angle of inclination

ΔZ vertical component of the earth field

IGRF International Geomagnetic Reference Field

RTP Reduced to the Pole

1VD First vertical Derivative G

Gravitational constant g

Acceleration due to gravity V

Gravitational potential

c.g.s Centi gram second

g.u gravity unit

IGSN International Gravity Standardization Network

GPS Global position system $g_{Ø}$ Predicted

gravity at a potential latitude Ø

Ø Latitude ρ

Density

BC Bouguer Correction nT

nanoTesla r Distance h

Orthormetric height

DEM Digital elevation model

Π Pi

Acknowledgment

I thank the almighty God for seeing me through this whole project with His love, courage and strength.

I am very grateful to Mr. Kwaku Takyi Kyeremeh, regional geophysicist at Newmont Ghana Gold Limited who also doubles as my supervisor for making this research come into fruition. Thank you for making accessible geophysical equipment, time taken in Oasis montaj and Arc GIS software training and your kindness. Many thanks also go to the staff at the Geophysics department at Newmont

Ghana Gold Limited for their warm welcome, assistance and patience especially Amos and Seth. Great thanks also go to my cheif supervisor Dr. Isaac Dadzie for his guidance, patience and inspiration. Big appreciation goes to all the staff at the geological engineering department especially Prof. S.K.Y Gawu, Dr. Ali and Dr. E. Appiah-Adjei for their encouragement and kindness. To my colleagues especially Albert Asare, I say a very big thank you for your motivation. Special regards to my mum Adwoa Omenaa, my sisters Jackline, Lina and Nina and my brother in-law Mr. Kwabena Wereko, I say God bless you for all the support you provided throughout the process.

CHAPTER ONE

INTRODUCTION

1.1 Background

Ghana falls in the West African Craton with most of its primary gold lodes occurring in deep-seated shear zones that have been controlled by local unconformities between the Birimian metavolcanics and metasediments (Kesse, 1985). Among the five northeast trending volcanic belts in Ghana is the Sefwi belt with large gold deposits on the southeast and northwest margins. Primary gold occurs along the structures that form the sheared margin of the belt. The gold is probably of syngenetic volcanic origin related to greenstone volcanism and associated sedimentation, remobilized during the Eburnean orogeny to become concentrated and localized along major shear (Griffis et al., 2002).

Gravity and magnetic geophysical survey have been extensively used for mineral exploration to aid in delineating metaliferous ores (Airo & Mertanen, 2008; Hinson et al., 2015). In order to have an observable response, the geophysical method applied requires a difference in the target of interest and the surrounding rock in terms of their physical properties. Potential field methods (gravity and magnetic) are capable of delineating the subsurface geology in terms of lithology, geological structures and hydrothermal altered zones especially in structurally guided mineral zones where contrast in density and magnetic susceptibility help yield better results.

In order to enhance exploration techniques and reduce cost of drilling, geophysical tools including potential field methods which are comparatively cheaper and faster in operation are resorted to.

Magnetic data was used to characterize the structural control on gold at the Central Lapland greenstone belt , Finland (Airo & Mertanen, 2008). Gravity survey was used to investigate the structurally guided W-Sn mineral resource related to granites in Nanling Range of South China (Chen et al., 2015). Again aeromagnetic data was interpreted to detect a possible gold mineralization in Kyerano on the Sefwi belt of Ghana. This was achieved by determining lithological boundaries, geological structures and hydrothermal altered zones linking to mineralization (Wemegah et al. 2015). Aeromagnetic and aerogravity survey data were integrated to investigate the mineral potential of a section of the Volta Basin of (Hinson et al., 2015).

1.2 Problem statement

The Hwediem concession in the Ahafo district of Ghana in the Sefwi belt has prominent structurally controlled gold mineralization. The area is characterized by pockets of small scale gold mining operations (Galamsey) which have no concrete mapped trend of gold mineralization. Previous geological exploration surveys have detected anomalous zones of gold mineralization. Geophysical tools are relied upon to enhance the exploration program and reduce the cost of drilling. Due to the detection of sulphides (chargeable) and quartz veins (electrically high resistive) from previous survey, induced polarization (IP) and pole dipole geophysical methods were carried out respectively. The results of the IP and the resistivity survey could not clearly define the anomalous pattern due to the complex nature of the mineralization in the area.

Subsequently, due to the unsatisfactory results from the IP and resistivity, this research resorted to potential field geophysical survey (gravity and magnetics) with the view that contrasts in magnetic susceptibility and density will be helpful in mapping out the different lithological units, define geological structures and delineate any possible gold mineralization zones.

1.3 Justification

There have been instances in Ghana suggesting that exploration activities are discontinued because of the inability to detect feasible gold mineralization for further studies especially where conventional methods of gold exploration were used (Griffis et al., 2002). As exploration for mineral deposits becomes hard, geophysical methods are growingly depended on to help locate mineralization areas (Bishop & Emerson, 1999). Magnetic and gravity geophysical survey work best for lithological mapping, locating hydrothermal altered zones and geological structures linked with mineral deposit. With regards to the study area in the Sefwi belt, contrast in rock density and magnetic susceptibility could help to delineate structurally controlled mineralization.

1.4 Objectives

The primary aim is to integrate ground magnetic and gravity geophysical methods to delineate potential gold mineralization at the Hwediem prospect - Sefwi belt. To achieve this goal the following specific objectives need to be achieved from the geophysical anomaly maps that will be produced;

- Lithological mapping of the study area
- Map geological structures capable of hosting gold mineralization
- Map and relate small scale mining sites (Galamsey) to the outcome of the geophysical survey.

1.5 Study area

1.5.1 Location and Accessibility

The survey area falls in the southwestern portion of Ghana, a town called Hwediem in the Asutifi north district of the Brong Ahafo region (Figure 1.1). The district is situated between latitudes 6°40‘ and 7°15‘ North and longitudes 2°15‘ and 2°45‘ West. Hwediem is close to Kenyasi; the district capital which is about 50km from Sunyani, the capital of Brong Ahafo region. The study area is accessible by the unpaved Kenyasi-Ntotoroso road.

1.5.2 Climate, Topography and Vegetation

The area is characterized by two main rainy seasons and falls within the wet semiequatorial belt with comparatively abundant rainfall. The first season commences around March, reaches its apex in June and falls off in July; the second season covers mainly September to October. The months of November through February are dry. In terms of topography, the survey area is relatively level with elevation that ranges from 182 to 228m above mean sea level. The survey area is covered with shrubs and grass which serves as farm land for the local community.

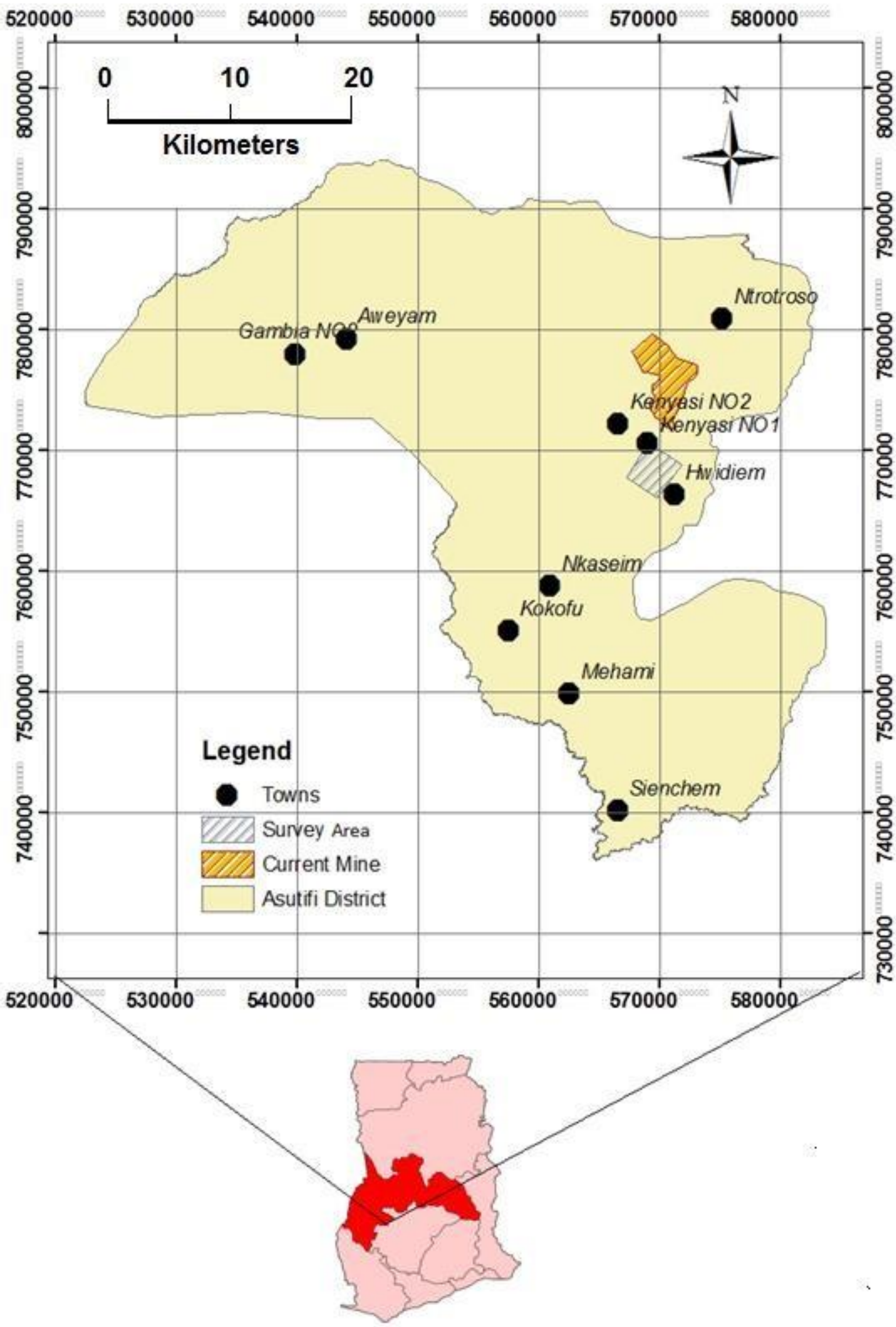

Figure 1.1: Location Map of Study Area

CHAPTER 2 GEOLOGICAL SETTING

2.1 Regional geology

Geologically Ghana is located in the confines of the eastern portion of the Man Shield covering the southeastern part of the West African Craton. The folded and metamorphosed Birimian, Buem formation, Tarkwaian, Voltain, Dahomeyan system and the Togo series are the major rock assemblages in the country (Kesse, 1985). Paleoproterozoic rock units comprise of the Tarkwain and the Birimian Super Group with the latter referred to as the most important and extensive unit of the Man Shield which is about 2.1 to 2.2Ga in age (Griffis et al., 2002). During the Eburnean orogenic event, these two groups of rock units were metamorphosed to greenschist facies grade. Extensive gold mineralization in the paleoproterozoic of the southwestern portion of Ghana is also related to the orogenic event.

2.1.1 Birimian Supergroup

The Birimian in Ghana which largely covers the southwestern part of Ghana is subdivided into two main groups; the Birimian metasediments and the metavolcanics (Leube et al., 1990). The Birimian metasedimentary rocks are made up of volcaniclastic rocks, argillitic rocks, wackes related to turbidites and sediments derived from chemicals (Leube et al., 1990).

The Birimian metavolcanics comprise several northeast southwest trending volcanic belts of tholeitic to acidic composition. These volcanic belts include; Kibi-Winneba, Sefwi, Ashanti, Bui, Bole-Nangodi, and the Lawra belts (Figure 2.1). In the extreme northwestern of Ghana is the Lawra belt which is the only belt that exhibit Northsouth trend (Leube et al., 1990). Separation between individual belts is dominated by metasedimentary rocks which are folded and granitoids occurring in disproportionate amount as shown in Figure 2.1

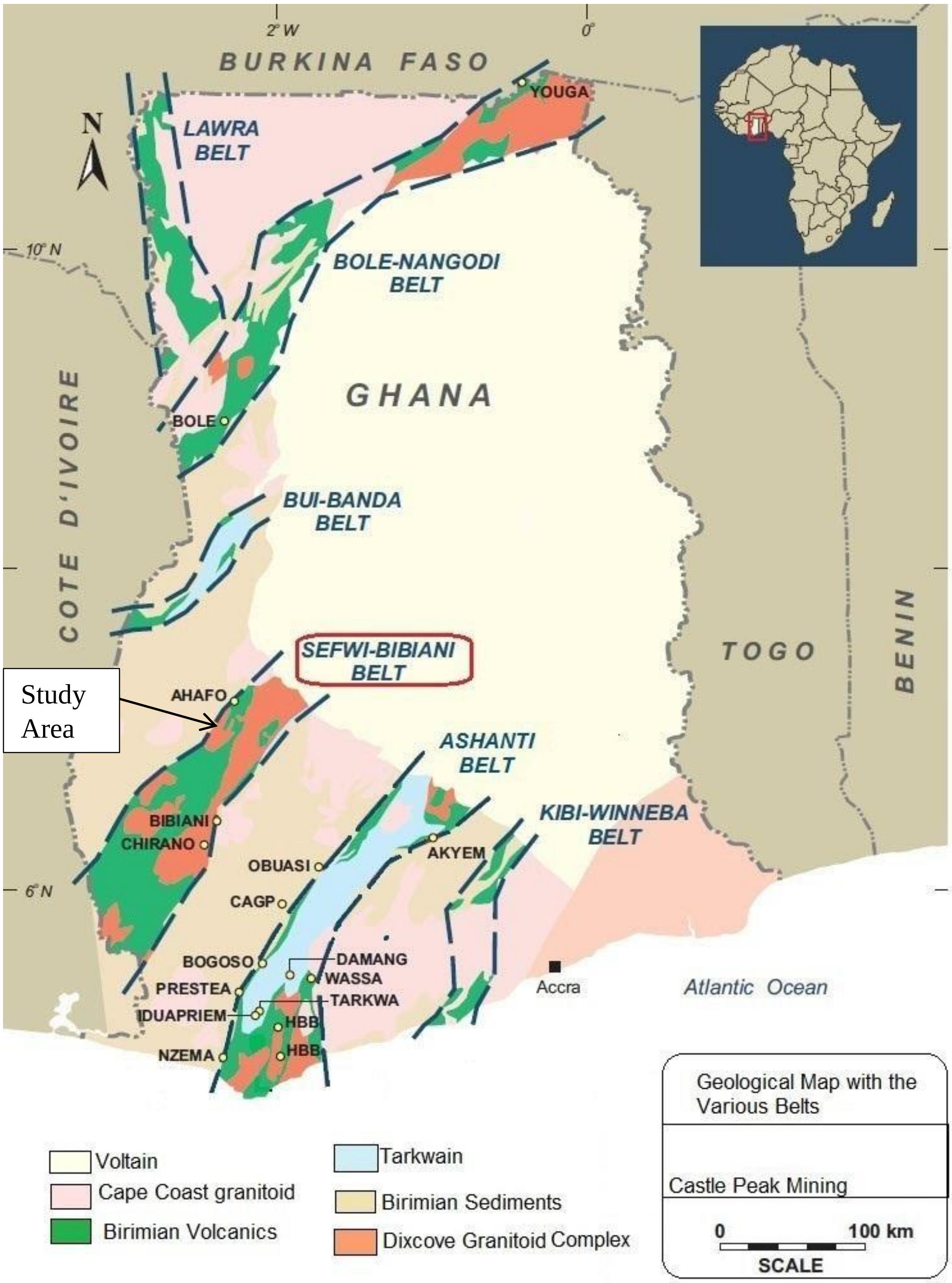

Figure 2.1: Geological Map of Ghana showing the various Volcanic Belts

2.1.1.1 Birimian Granitic Intrusions

A large variety of granitoids intrudes paleoproterozoic Birimian volcanic belts and the various (Yao & Robb, 2000; Oberthor et al. ,1996). Two major types of granitic intrusions have been recognized in several parts of the Birimian of Ghana. The belt type (Dixcove) granitoids occur mainly within the confines of the volcanic belts. They are dioritic to granodioritic in composition with hornblende usually as the dominant mafic mineral (Griffis et al., 2002; Oberthor et al., 1996).

The basin type (Cape Coast) granitoids are granodioritic to granitic in composition with biotite as the major mafic mineral. They display foliation and are confined in areas where Birimian metasediments are widespread (Griffis et al., 2002; Yao & Robb, 2000; Oberthor et al., 1996).

2.1.2 Tarkwaian

This rock formation is made up of a distinctive sequence of the metasediments occurring within a broad band along the interior of the Ashanti belt and which host important paleoplacer gold deposits in the Tarkwa district of Ghana (Griffis et al., 2002). The sediments are mainly of shallow water continental origins and contain fragments acquired from the Birimian (Junner, 1935). The Tarkwaian is said to rest unconformably on the Birimian in some places in Ghana which appears in general less strongly deformed and metamorphosed than the Birimian (Griffis et al. 2002). The Tarkwaian comprise of a variety of sandstones, conglomerate and argillites deformed and metamorphosed under greenschist facies conditions during the Eburnean orogeny (Oberthor et al., 1996).

2.1.3 Regional Scale Gold Deposit of Ghana

Kesse (1985) classified gold deposits in Ghana into three main broad suites which include;

1. Birimian-hosted deposits
2. Tarkwaian-hosted deposits
3. Modern alluvial deposits

2.1.3.1 Birimian-Hosted Deposits

These type of deposits are generally associated with composite quartz-veins arrays which are usually related to disseminated sulphides (Kesse, 1985). They include most of the important lode/vein deposits in Ghana such as Obuasi, Bogosu, Prestea, Chirano, Konongo and Ahafo gold deposits in Ghana (Griffis et al., 2002). They are usually related to NNE to NE regional structures. The likely host rocks are greywackes, argillites, and volcaniclastic rocks. Besides, important host rocks recognized are intermediate and mafic granitic intrusions occurring in the volcanic belt (Ahafo Mineral Resource/Reserve Report, 2006). Quartz vein systems which cut across are closely related to broad zones of disseminated sulphides in the host rocks. The disseminated sulphides consist mainly of pyrite and arsenopyrite in variable amount with gold associated with arsenopyrite being complex in nature (Griffis et al., 2002; Kesse, 1985).

2.1.3.2 Tarkwaian-Hosted Deposits

These deposits are made up of auriferous quartz pebble conglomerates although at the north of Tarkwa, Damang exploits sheeted quartz-vein stockwork hosted deposit in Tarkwaian sediments. The banket formation overlying the Kawere is economically the most important member of the deposit.

The main Tarkwaian-hosted deposits are confined to the Tarkwaian system (Griffis et al., 2002).

2.1.3.3 Recent Alluvial Deposits

They are derived mainly from the primary vein and lode type deposits associated with the Birimian system (Kesse, 1985). Although this is a major source of the historical gold production, commercial scale alluvial mining is in decline and is likely to remain so as a result of environmental constraints (Griffis et al., 2002; Ahafo Mineral Resource/Reserve Report, 2006).

2.2 Local Geology

2.2.1 Sefwi Belt

The Sefwi volcanic belt is among the SW-NE trending belts located in Ghana (Figure 2.1). It is surrounded to the southeast by the Kumasi basin and to the northwest by the Sunyani sedimentary basin. It stretches for about 40-60km of width with many gold occurrences. Metasediments, mafic volcanic and appreciable belt-type intrusive rocks dominate the belt (Griffis et al., 2002).

Griffis et al. (2002) divided the Sefwi belt into four margins based on geographical areas;

1. The NE margin (North Bibiani Range): This margin covers largely the north eastern portion of the Sefwi belt and partly into the adjacent Kumasi basin. Birimian metasediments, metavolcanics and belt-type granitoids are widespread in the area. The metasediments are mainly made of argillites and greywacke with interbedded volcaniclastic and volcanics. Basalt, rhyolite flows, chert and tuff with interbed of argillite make up the Birimian

metavolcanics. Belt-type granitic intrusions are also widespread with isoclinal folding, NE trending faults making the variable structures in the area. Birimian metavolcanics, metasediments and also granitoids serve as host for gold mineralization which is structurally guided.

2. NW Margin (North Goaso area): This margin falls in the northwestern of the Sefwi belt and also partly into the adjacent Sunyani basin. This portion consists of intermediate belt-type granitoid batholiths that intrude extensive mafic metavolcanics. A section of the margin is also dominated by marine sediments varying from greywacke complexes to high volcaniclastics and argillaceous components. The major structural feature is the northeast to southwest trending regional fault that divides the belt-type granitoids, metavolcanics and the adjacent Sunyani basin locally termed as the Kenyasi Thrust. In addition E-W and NW-SE crosscutting features are also dominant. Complex structural systems chiefly guide the gold mineralization in the area.
3. SW Margin (Juabeso-Bia West Tanoso): This portion covers the south western half of the Sefwi belt and also part of the eastern margin of the adjacent Sunyani basin. Mafic volcanics and composite intrusive sequences cover the eastern and western part of the margin with the interior portion covered by metasediments. Intermediate intrusive complexes relating to the belt-type granitoid which feature large roof pendants intrude the metavolcanics and metasediments. Several NW and N-S trending suites of small cross faults are widespread which may have controlled a lot of gold mineralization.
4. SE Margin (Enchi): The margin covers the south eastern portion of the Sefwi belt. Thick series of Birimian mafic volcanics are prevalent in the area with

the major belt of gold mineralization occurring east of the mafic volcanics in an area covered mainly by Birimian volcaniclastics and metasediments. Gold mineralization associated with vein systems is also related to fairly NE trending faults.

2.2.2 Geology of the Study Area

The study area (Hwediem Prospect) falls in the northwestern margin of the NE trending Sefwi volcanic belt. Generally the geology and mineralization trend of the Hwediem prospect is likened to the Subika deposit (also in the northwestern margin of the Sefwi belt) which geologically exhibit uncommon mineralization style in this section of the Sefwi belt; occurring within intrusives and controlled by geological structures falling off the major structure (Kyenyasi Shear Zone) in the area (Ahafo Mineral Resource/Reserve Report, 2006).

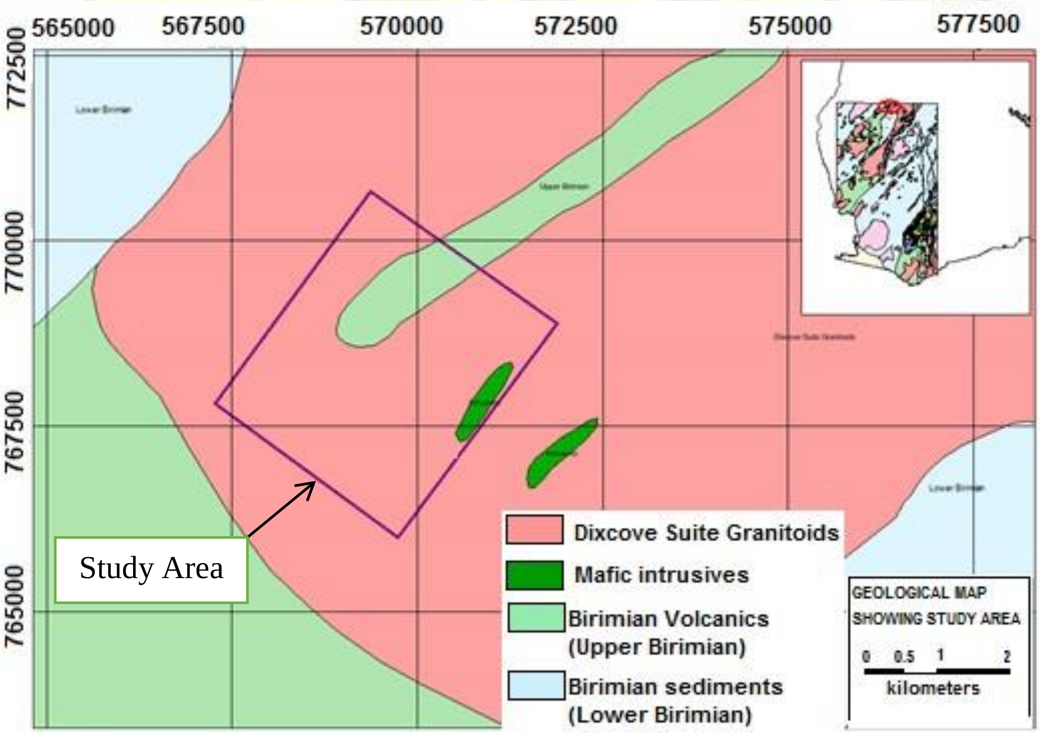

Figure 2.2: Geological map of the study Area

2.1.1.1 Lithological Units

At a regional scale, the main lithological units mapped in the area are grouped under one unit referred as The Granitoid Units (GD). This is a wide variety of rock units dominated by the Birimian belt-type granitoid units along with the Birimian volcanic facies and mafic intrusive units. The GD is greenschist to lower amphibolite metamorphic grade and have been subdivided into individual units mainly Diorite, Gabbro, and granodiorite (Ahafo Mineral Resource/Reserve Report, 2006).

2.2.2.2 *Mineralization and Alteration*

Gold mineralization in the study area regionally falls under the Birimian-hosted deposit type and is suspected to be focused in intensely altered fracture zones, generally a zone of brittle fracture with a lot of quartz, Fe carbonate pyrite veins and veinlets. Gold mineralization is largely controlled by the distribution of fracturing and veining in host rocks. Quartz and carbonated veinlets are believed to form stockworks which are sometimes filled with pyrite and visible gold in some instances. Veining and mineralization are associated with silica albite and Fecarbonate. The nature of mineralization is suspected to be related to the occurrence of a number of dykes which are present in most mineralized connections. The dykes can be mineralized if they contain quartz Fe-carbonate veins (Ahafo Mineral Resource/Reserve Report, 2006).

The grade of mineralization is generally related to the intensity of alteration. Alteration is proposed to be characterized by slightly bleaching of granitoid (GD) due to chlorite alteration; breakdown of ferromagnesian phase. Another form of alteration develops sericite and weak silica (Ahafo Mineral Resource/Reserve Report, 2006)

CHAPTER THREE THEORETICAL BACKGROUND

3.1 Magnetic Method

The magnetic method is a potential field geophysical technique. It is hinged on the fact that variations of the passive magnetic field which result from the magnetic susceptibility difference of the underlying rock can be used to investigate the subsurface geology. Magnetic method remains the oldest, cheapest, widely used and dependable geophysical method for locating structures and minerals relating to ore deposit (Sharma, 1987).

3.1.1 Basic Concept and Definitions

The earth behaves like a magnetic body surrounded by potential field lines. Magnetic poles always occur in pairs, the North Pole (positive) pole and the South Pole (negative).

3.1.1.1 Magnetic Force F

If a distance r sets two magnetic poles of strength m_1 and m_2 apart, then the magnetic force F that is between them is given as;

$$\mathbf{F} = \frac{m1m2}{4\pi\mu r^2} \tag{1}$$

Where μ is the **magnetic permeability** of the medium between the poles

3.1.1.2 Magnetic Units

Around a bar of magnet a magnetic flux which is produced by a magnetic field strength **H** exists, the flux per unit area is the flux density denoted as **B**. The flux density **B** which is a vector quantity is sometimes referred to as magnetic induction and is measured in werber/m^2 or in Tesla [T]. In geophysical work a subunit nanoTesla is used because Teslas are too large in practice. The flux density **B** is defined as

$$\mathbf{B} = \mu\mathbf{H} \qquad (2)$$

Where μ is the absolute magnetic permeability of the medium on which the magnetic field strength **H** is acting. For any non-magnetic body (water and air), $\mu=\mu_o$ where μ_o is the permeability of vacuum which has the value of 4×10^7 wb/Am. For any medium other than vacuum, $\mu = \mu_r\times \mu_o$ where μ_r is the relative permeability. Since $\mu= \mu_r\times \mu_o$

$$\mathbf{B} = \mu_r\mu_o\mathbf{H} \qquad (3)$$

Rearranging and introducing magnetic susceptibility $K=\mu_r-1$; flux density **B**=

$$(k+1)\ \mu_o\mathbf{H}$$

$$\mathbf{B} = k\mu_o\mathbf{H}+\mu_o\mathbf{H} \qquad (4)$$

Magnetic susceptibility is a constant of proportionality for any magnetizable body and can be measured in the field and laboratories for rocks.

In vacuum $\mu_r=1$ and K=0 and as such equation (4) reduces to equation (2). Apart from vacuum any other media have an extra magnetizing field called the intensity of magnetization **J** [A/m] which is induced by **H**.

$$\mathbf{J} = k\mathbf{H} \qquad (5)$$

Equation (2) can be generalized, according to Parasnis (1979), as

$$\mathbf{B} = \mu_o\mathbf{H}+k\mathbf{J} \qquad (6)$$

The earth magnetic field is denoted as **F** and corresponds to **B** in equation (6). In magnetic survey, B corresponds to the measured field which is made up of the earth‘s field and a secondary field induced by the magnetic minerals such as magnetite and pyrrhotite.

3.1.2 Diamagnetism, Paramagnetism and Ferromagnetism

Provided that two electrons spin in opposite direction, then the two electrons can be accommodated by the same electron shell according to quantum theory. The magnetic moment of two such electrons called paired electron will cancel out.

In diamagnetism, all the electron shells are completely occupied such that no paired electrons exist. The rotation of the electrons produces a magnetic field opposing the applied field. These result in weak, negative magnetic susceptibility. Examples of such materials are Halite and quartzite (Reynolds, 1997).

Paramagnetic materials have incomplete electron shells in such a way that rotation of their unpaired electrons in an exterior field generates magnetic field with a positive susceptibility that is relatively weak.

Ferromagnetic minerals are paramagnetic although they have clusters of atoms that align to form domains. The value of **k** is higher in ferromagnetic minerals than paramagnetic materials (Kearey et al., 2002). For ferromagnetic materials, the magnetization by strong magnetic field follows a hysteresis loop as shown in Figure 3.1. If the applied field remains strong enough then the magnetization reaches a saturation point $\mathbf{J_S}$, beyond which any extreme accretion in the field causes no extra addition in magnetization. When the H-field is reduced after saturation, some magnetization last referred to as remenant magnetization. To get rid of the remnant magnetization, a negative H-field, $\mathbf{H_c}$ has to be applied (Sharma, 1986). Ferromagnetism decreases with an increase in temperature and it is wholly lost at Curie temperature. Examples of ferromagnetic materials include substances such as cobalt, iron, and nickel (Telford et al., 1990).

Antiferrimagnetic minerals have domains divided into regions that align in opposite direction so that moments nearly cancel out as shown in Figure 3.2. An example is iron oxide hematite (Fe_2O_3). *Ferrimagnetic materials* have regions that are lined up to oppose each other in such a way that one direction is stronger in strength against the other as shown in Figure 3.2. Practically virtually all magnetic minerals fall under this category. Examples include magnetite (Fe_2O_3), titanomagnetite, ilmenite and the oxides of iron or iron and titanium.

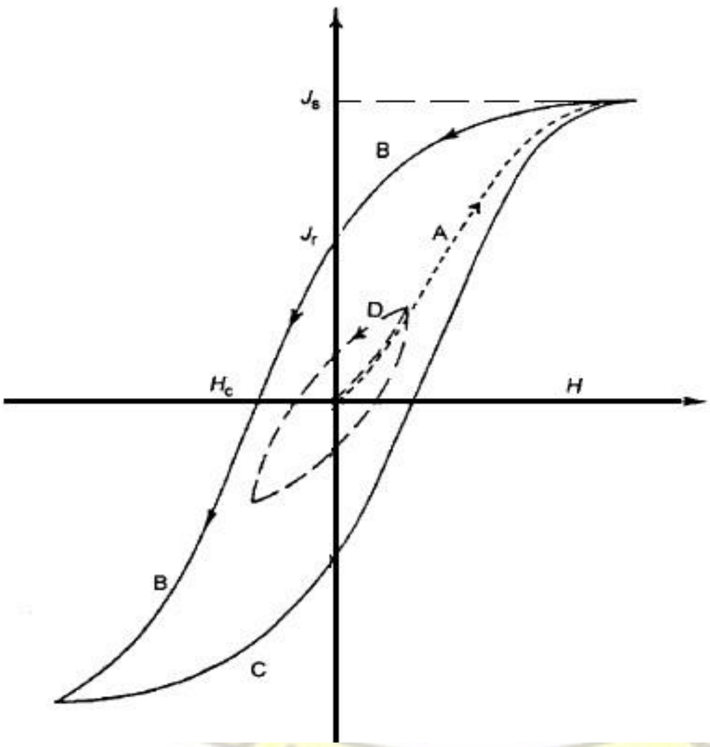

Figure 3.1: Hysterisis loop illustrating the cycle of magnetization cycle at saturation curves A, B and C. Curve D shows magnetization without saturation (Sharma, 1986).

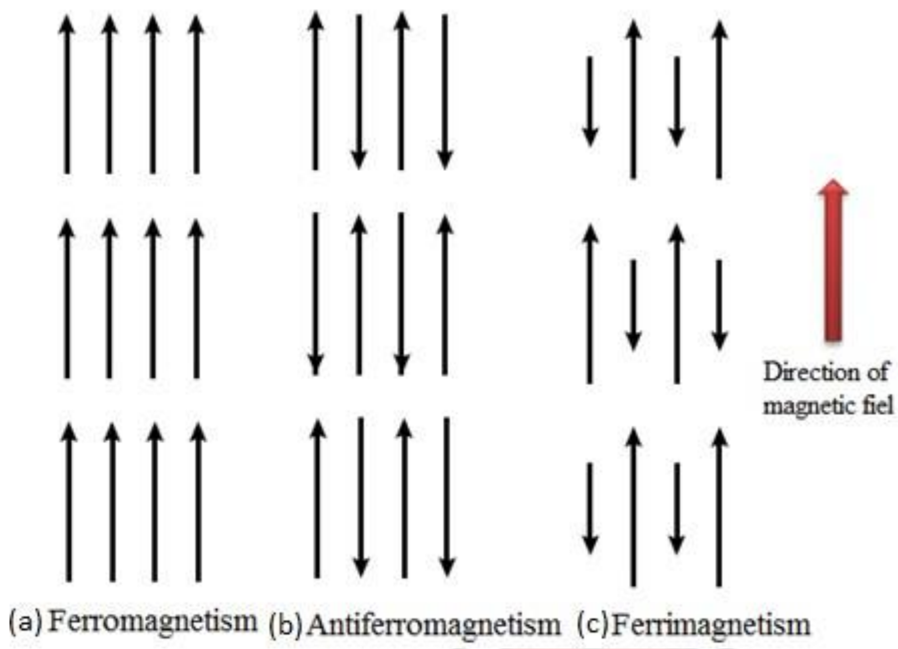

Figure 3.2: Representation of magnetic moments in atoms of different materials (Kearey et al.,2002)

3.1.3 Magnetic Susceptibility of Rocks

Magnetic susceptibility **k** is analogous to density in gravity surveying. It is the measure of how magnetizable a material is. Rocks with high content of ferromagnetic minerals tend to have the highest susceptibility. Because of the high content of magnetite in basic igneous rocks, they possess the highest magnetic susceptibilities. Magnetite content reduces with increase in rock acidity and hence **k** is small in high silica content rocks such as granite. In general, susceptibility values for metamorphic rocks range from fair to low with sedimentary rocks having a very small susceptibility values (Kearey et al., 2002).

3.1.4 Remanent Magnetization of Rocks

Remanent magnetization is the magnetization caused by earlier events of the rock and can be acquired by primary and secondary processes. Primary remnant magnetization is acquired in most igneous rocks during formation when they cool through the Curie temperature of its minerals (thermo remnant magnetization) (Parasnis, 1979). Primary remnant magnetization in sedimentary rocks is gained as grains slowly settle in the presence of the earth field (Parasnis, 1979; Telford et al., 1990). Secondary remnant magnetization in rocks is attained after its formation such as during metamorphism and chemical grain alteration of rock minerals (Reynolds, 1997).

3.1.5 Earth Magnetic Field

In magnetic survey the total magnetic intensity measured is composed of

(1) The main field: this can be approximated to a dipole field inclined about 11.5° to the earth‘s rotation axis which can be modelled as polar and equatorial dipoles (Reynolds, 1997; Kearey et al., 2002). In the absence of any other magnetic field, a freely hanged magnetized needle, will assume a direction of the total geomagnetic field. The main field is a vector described by the geomagnetic elements (Figure 3.3). The magnitude of the total field vector **B** has a vertical component **ΔZ** and a horizontal component **H** in the direction of the magnetic north. The dip of **B** is represented as the inclination **I** and the declination **D** is the horizontal angle the geographic north makes with the magnetic north. Generally, the strength of **B** varies from 2500 nT at the equator to 70000 nT at the poles (Telford et al., 1990; Kearey et al., 2002). The earth‘s field (about 99%) is produced by convection in the outer core of the earth which pushes electric current (Telford et al., 1990).

(2) External field: This is the field due to the additional 1% of the earth field. It is due to electric currents found in the ionized layers of the exterior atmosphere.

It results in diurnal variation caused by compression of the earth‘s field on the sunward side, which varies with latitude and season (Nabighian et al., 2005; Telford et al., 1990).

(3) Local Magnetic anomalies: This constituent of the earth‘s field is produced by magnetic minerals in the crust where the temperature is lower than 580°C (Curie temperature of magnetite). The information this anomaly provides is the target of magnetic surveys (Nabighian et al., 2005).

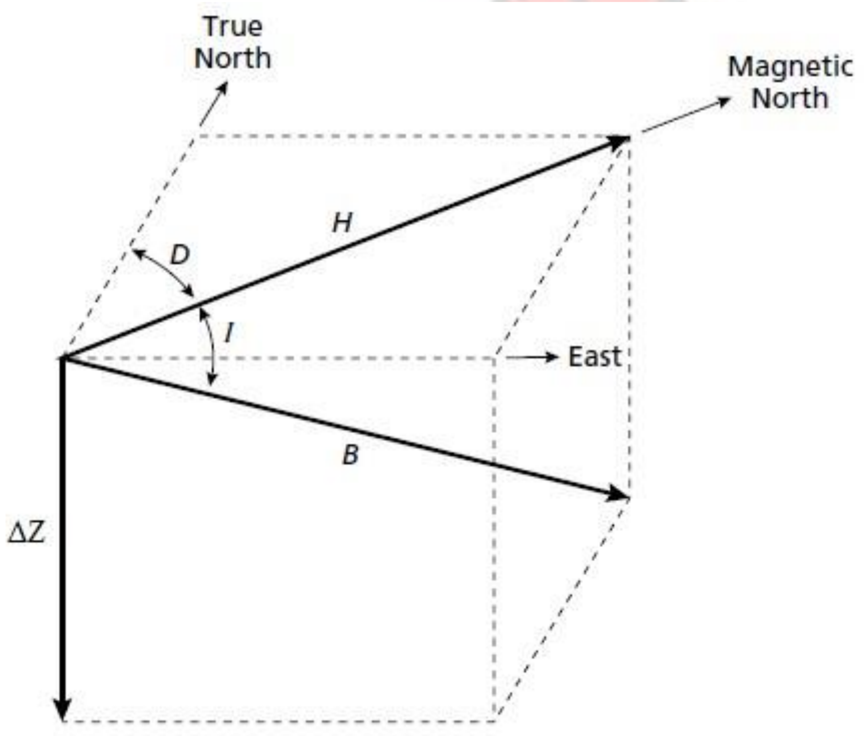

Figure 3.3: Elements of Geomagnetism (Kearey et al., 2002)

3.1.6 International Geomagnetic Reference Field (IGRF)

The spatial distribution and theoretical unperturbed total magnetic field at each point on the earth have been calculated using spherical harmonic analyses. This field is termed as the international geomagnetic reference field which is published every five years. In magnetic survey, the IGRF is helpful in taking out any variations due to the theoretical field from the observed magnetic data (Reynolds 1997; Kearey et al., 2002).

3.1.7 Magnetic Data Reduction

Magnetic data reduction is done to remove all factors causing variations in the observed magnetic intensity with the exception of the variations due to magnetic minerals in the subsurface. The major corrections applied to the observed magnetic data are diurnal variation correction and geomagnetic correction (Kearey et al., 2002).

3.1.8 Magnetic Data Enhancement

Magnetic data enhancements comprise of techniques and filters used on the reduced observed magnetic data to aid interpretation. The actual goals for applying these enhancing filters vary depending on the situation at hand (Nabighian et al., 2005). Fourier transforms are helpful in filtering magnetic data (Telford et al., 1990). Among other filters and enhancing techniques applied on magnetic data are reduced to Pole (RTP), first and second derivatives, analytical signal, upward and downward continuation.

3.2 Gravity Method

Gravity survey is a potential field geophysical method that includes the measurement of variations in the earth‘s gravity field at designated positions and interpreting the variations in the measured gravity to estimate the depth, geometry and density of the causative body. The success of gravity survey largely depends on the contrast in bulk density (mass) of the different earth materials that result in variations in the measured gravity field. This method has been useful in oil and gas explorations though many other applications have been found including mineral exploration.

3.2.1 Basic Principles

The basis for the gravity method is the Newton‘s law of gravitation. This states that the force of attraction F, between any two substances of known masses m_1, m_2 is directly proportional to the product of the masses and inversely proportional to the square of the distance r between them. This is given as

$$\mathbf{F} = G\frac{m1\mathrm{m}2}{r^2} \qquad (7)$$

Where G is the gravitational constant=6.67×10^{-11} Nm^2kg^{-2}.

Newton‘s law of motion states that a force (F) is equal to the product of mass (m) and acceleration. It is due to gravity (g) if the acceleration is in a vertical direction.

$$\mathbf{F} = \mathrm{m}\mathbf{g} \qquad (8)$$

By combining the Universal law of gravitation with Newton‘s law of motion, the acceleration of m

$$\mathbf{g} = \frac{\mathbf{F}}{\mathrm{m}} = \frac{\mathrm{GM}}{R^2} \qquad (9)$$

Where g is known as the acceleration due to gravity, M is the mass of homogeneous earth and radius R.

This shows that on the surface of the earth, the magnitude of acceleration due to gravity (g) is directly proportional to the mass M of the earth and inversely proportional to the square of the radius of the earth, R if r=R. The acceleration due to gravity varies over the earth and this variation is attributed to the flattened spherical shape resulting from the imbalance between gravitational field and the centrifugal force of attraction.

3.2.2 Gravitational Potential

Gravitational potential **V** is the work done by the force field resulting from a mass M to move a unit mass from a point distance *r* from M to infinity.

$$\mathbf{V} = \int_r^{\infty} \boldsymbol{F}\, dr = \frac{GM}{r} \tag{10}$$

Gravitational potential (**V**) is a scalar quantity and is an additive potential. It is a function whose derivative is gravitational force **F.**

$$\frac{dV}{dr} = - \frac{GM}{r} = F \tag{11}$$

Equipotential surfaces can be marked on which **V** is invariable. The geoid is the major equipotential surface which is perpendicular to the direction of gravity (Kearey et al., 2002). Another reference surface which does not coincide with the geoid and similar to the form of the earth is referred to as the reference spheroid.

3.2.3 Gravity Units

At the surface of the earth, the average value of gravity measured is about 9.8 ms^{-2}.

The c.g.s unit of acceleration due to gravity (1cm/s^2) is Gal in honor of Galileo. Recent gravimeters are very sensitive and can measure gravity values as low as 1 part in 10^9. This has resulted in the use of sub-units like milliGal and microGal in gravity measurements. The SI unit of acceleration due to gravity is known as the gravity unit (g.u.), where 1 g.u. is equivalent to 0.1 milliGal. MilliGal and microGal are generally used because the gravity unit has not been accepted all round (Reynolds, 1997).

3.2.4 Density of Rocks and Minerals

Density is the main physical property for gravity method. Anomalies recorded in gravity survey are as a result of the lateral variations in density of rocks. Porosity and mineral composition are major factors that affect the density of rocks. Usually direct density measurements are made in the laboratory on rock samples. The results may not give the true bulk density due to the fact that in the process of obtaining the samples, they may have been weathered, dehydrated or altered (Telford et al., 1990).

Difference in porosity in sedimentary rocks is the major factor for changes in density. In igneous rocks, composition is the main determinant of density variation although there is overlap of density (Figure 3.4). Generally igneous rocks are denser than sedimentary rocks. Density commonly increases with a decrease in silica content; thus basic igneous rocks are denser than acid rocks. Metamorphic rocks exhibit a density increase with an increase in grade of metamorphism and with fall in acidity (Kearey et al., 2002; Reynolds, 1997).

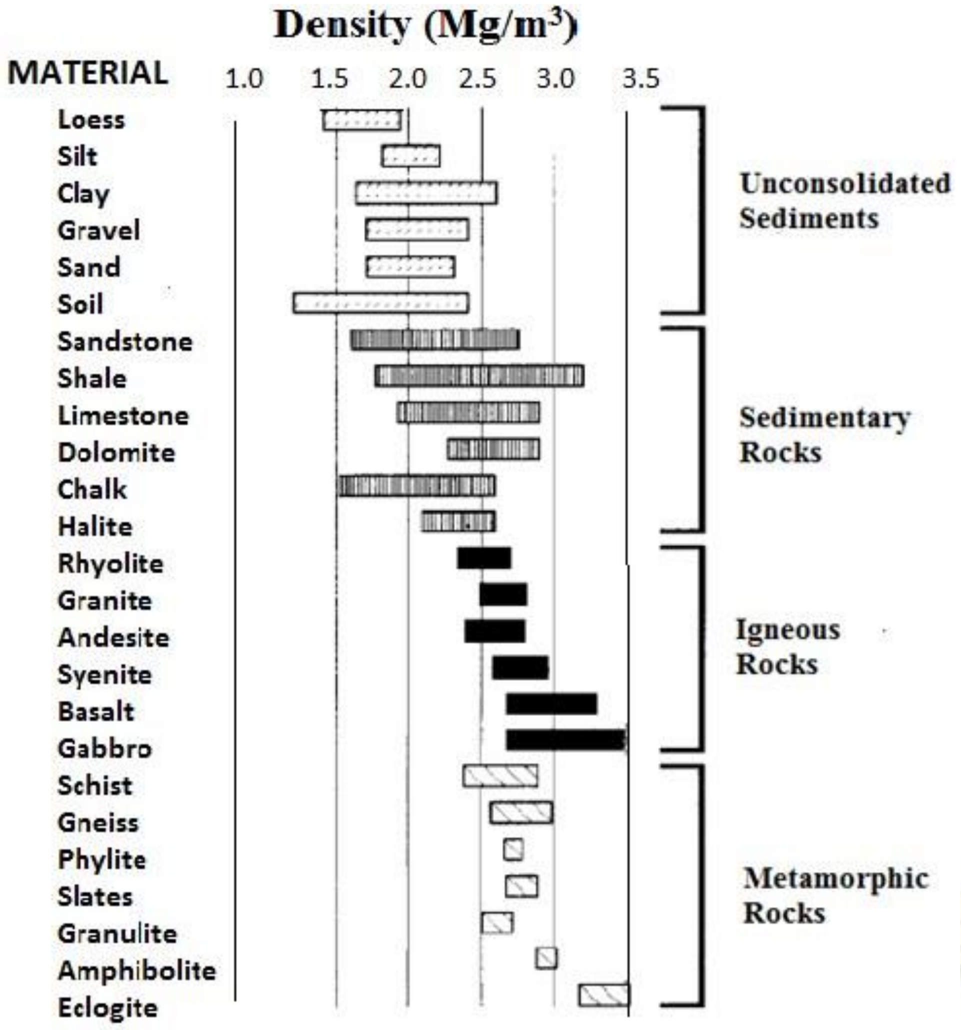

Figure 3.4: Density variations for different types of Rocks (Reynolds ,1997).

3.2.5 Gravity Measurements

Gravity is acceleration and for that matter goes with the measurement of time and distance in a specified direction. But with the high accuracy and precision expected in gravity surveying such elementary measurements are not easily attainable (Kearey et al., 2002).

The measuring of the absolute value of gravity remains an uneasy task which needs a careful and lengthy period of observations in complex experimental procedures. Such measurements are made using two main techniques; swinging pendulum and falling body. By referring to the International Gravity Standardization Network, 1971 (IGSN

1971), absolute gravity values at gravity stations can be acquired. The network composes of stations where absolute gravity has been measured (Kearey et al., 2002).

In gravity exploration survey, relative gravity, that is, the relative variation of gravity is measured using gravimeter. A base station is usually established first which can be related to the IGNS 71. All subsequent stations occupied during gravity survey are tied to the base station so that the survey is in a loop (Kearey et al., 2002).

3.2.6 Gravity Meters

Gravity meters or gravimeters are instruments with a high accuracy and sensitivity used to measure relative gravity. Generally the principle of operation of modern gravimeters depend on a constant mass attached to a spring balance; the change in length of the spring is related to the gravitational field at different locations (Kearey et al., 2002; Parasnis, 1979).

Generally two forms of gravimeters exist; stable and unstable gravimeters. Stable gravimeters are highly sensitive balances which measure the displacement of the spring balance from equilibrium when the force of gravity varies. The unstable gravimeters measure the force that is needed to put back the sensitive spring balance to equilibrium when displaced by variation in gravity (Parasnis, 1979).

3.2.7 Corrections to Gravity Observation

Before gravity data becomes interpretable in geological terms, corrections are applied to the gravimeter readings. Usually observed gravity is produced by multiplying the gravimeter reading by a calibration factor. The observed gravity data is reduced to an equipotential surface usually the mean sea level in order to isolate the variations due to density. This process is called gravity reduction to the geoid. The different corrections that are used include instrumental drift, earth tides,

Eotovos, free-air correction, Bouguer correction, Terrain and isostatic correction (Reynolds, 1997).

CHAPTER 4 MATERIALS AND METHODS

4.1 Magnetic Survey

Ground magnetic survey was carried out between the months of June and August with resources provided by Newmont Gold Ghana Limited.

4.1.1 Survey Design

For a deposit scale survey, the 3.6 km by 3.2 km survey area was mainly demarcated into a 100m traverse lines spacing; L6400 to L10000N (Figure 4.1) in order to cover the whole survey area. The direction of the traverse lines was set out at NW/SE which is perpendicular to the strike of the anomalous trend determined from the previous geological studies.

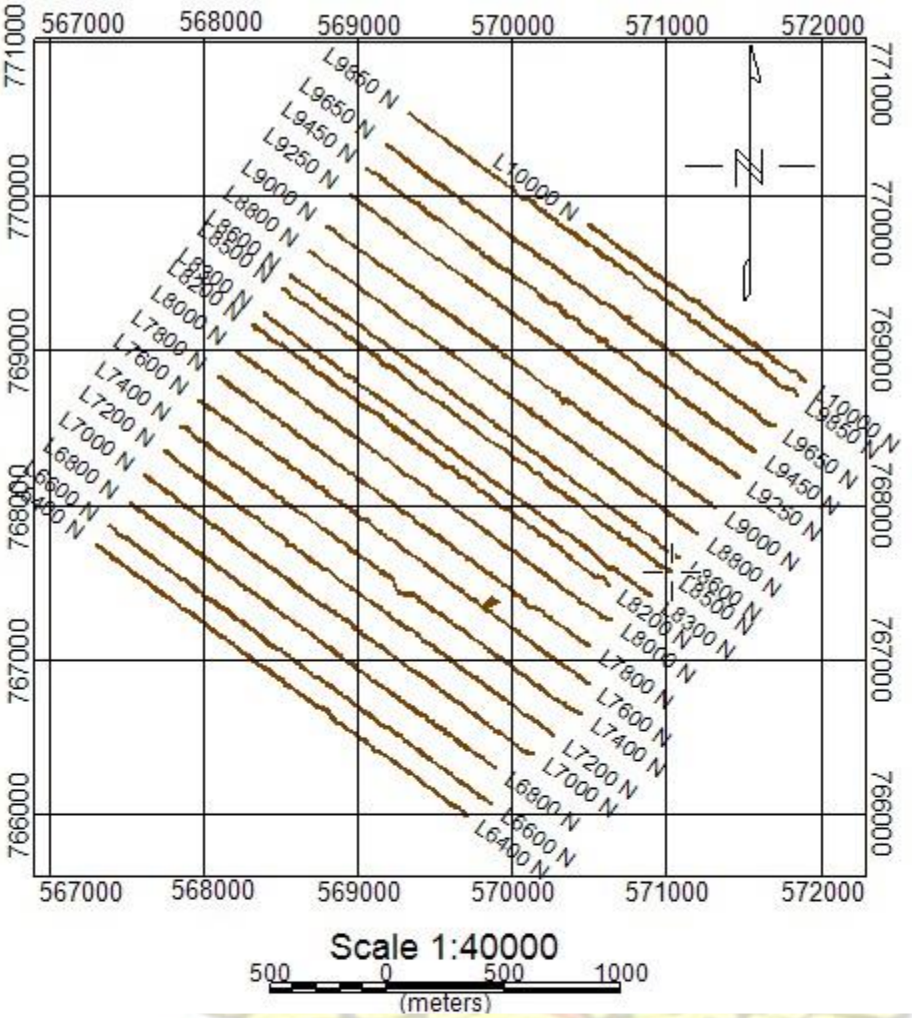

Figure 4.1: Magnetic Measurements along the NW/SE traverse lines (L6400-L10000)

4.1.2 Instrumentation

GEM‘s GSM-19 Overhauser magnetometer having resolution 0.01 nT and a complete accuracy of 0.2 nT was used for the data acquisition. It consists of a sensor containing a proton-rich fluid. A strong radio frequency is passed through a coil wound around the sensor which polarizes the proton-rich fluid. The proton magnetization is deviated by a short pulse into a plane of precession. A cut in the electrical current causes the polarized protons to precess in the earth‘s field and return to steady states after they have decayed slowly. The measured frequency is of the proton precession is converted into units of magnetic field.

4.1.3 Field Data Acquisition

Two magnetometers (GSM-19 Overhauser magnetometer) were used which were synchronized during the survey to obtain the lateral variation of magnetic susceptibility of the study area. Within the survey area, one was set up as a continually reading base magnetometer to check the effect of diurnal variations magnetic storms. The other magnetometer (rover) was put in a *WALKMAG* mode and carried as a backpack so that it continuously records (at sampling rates of up to every 1 second) magnitude of the total magnetic field (Sensor, labelled A in Fig 4.2) and positions (GPS, labelled D in Fig 4.2) of the data points along each traverse line.

In operating the magnetometer during the survey, it was ensured that metallic objects were not carried. Field notebook was carried along to record about any unavoidable magnetic interfering objects. The data was downloaded from the magnetometer and saved after each surveying day.

Figure 4.2: Magnetic survey in progress with Overhauser magnetometer. A- Control unit, processor and monitor, B- battery backpack, C-Sensor, D-GPS antenna (Photo: Seth, 2015)

4.1.4 Magnetic Data Reduction and Processing

These are quality assurance processes that are used to take out any noise attached to the data that are not associated with the subsurface geology. The following steps below were used to reduce the data to contain information that are relevant to the survey.

4.1.4.1 Diurnal Correction

Casual changes in the earth‘s magnetic field were corrected for by finding the difference between the time-synchronized signals measured at the base station magnetometer and the survey data (rover magnetometer). It was assumed that diurnal variation at the base station was same as the survey area.

4.1.4.2 Removal of Geomagnetic Reference Field

After correcting for the effect of diurnal variation, the observed magnetic field data was reduced to a residual value by removing the influence of the earth‘s main magnetic field from the survey data. The modelled international geomagnetic reference field for the survey area removed from the observed data was calculated using the IGRF extension in *oasis montaj* software.

4.1.4.3 Data Checking and Cleaning

A script was written with math in *oasis montaj* software by Geosoft Inc. to remove spurious noise and spikes from the data. Again the data was viewed in graphical profile form and spikes and outliers were manually removed. In order to obtain a more uniformly and a highly cleaned data, non-linear square filter was used to take out the remaining spikes and noise from the data.

4.1.5 Gridding

It is very difficult to collect magnetic data in a perfect traverse line and spacing. For a magnetic data in two dimensions, it is imperative to portray the data by finding its values at the various survey points that are evenly spaced at the nodes of grid.

A 25m cell size grid (one – fourth of the traverse line spacing) was created from the residual data (total magnetic intensity) with the help of the minimum curvature method (Briggs, 1974) in Gridding extension of the *oasis montaj* software. The gridded data was presented and displayed as an image. Gridding and interpolation of the data permitted the data to be visualized in a continuous form and also allowed image processing and data filtering.

4.1.6 Post Processing and Enhancement

A number of transformation techniques (liner filtering) are applied to the processed and gridded data (Milligan and Gunn, 1997). The mathematical enhancement techniques make anomalies less complicated and also allow attributes of a specific interest more pronounced at the expense of others. The filtering process is usually obtained when the Fourier transform of the data is increased in the frequency domain and converting the adjusted dataset back into the space domain and visualized (Milligun and Gunn, 1997).

All the filtering and enhancement techniques were automatically applied using the MAGMAP extension of the *oasis montaj* software. The filtering and enhancement techniques applied include Reduction to the Pole, Analytical signal and vertical derivatives as described below.

4.1.6.1 Reduction to the Pole

Magnetic field by induction recorded at low magnetic latitudes (close to the equator) is inclined and have anomalies asymmetric about its causative source. Reduction to the pole (RTP) changes the magnetic response to a field that would have been obtained at an inclination of 90°; that is the magnetic poles. The inducing earth's magnetic field tends to be vertical and anomalies are symmetric about their causative source at the magnetic poles (Milligun and Gunn, 1997). In magnetic survey, the RTP filter, which does not enhance noise is useful at identifying main litho-magnetic units and simplifies interpretation. The difficulty with RTP comes with incorrect computation in the presence of remanent magnetization and difficulty in computation near the magnetic equator.

The RTP filter was automatically employed on the gridded data (Total magnetic intensity) by making use of the numerical calculation presented by Baranov and Naudy (1964). The field parameters which enabled the data to be reduced to the pole include magnetic inclination and declination of -12.50 and -4.04 respectively and an average earth's field strength of 32293.609 nT. In order to have a stable Fourier domain transformation process, the residual field was first reduced to the equator. A factor of -1 was multiplied to the reduced to the equator grid which reversed the grid to the pole.

4.1.6.2 Analytic Signal

In areas of low magnetic latitudes where there is difficulty with the application of the RTP filter, the analytical signal filter becomes very useful. Nabighian (1972) developed the concept of analytical signal. Roest et al. (1992) define the analytical signal as a function that relates the magnetic field by the derivatives;

Analytical signal = $| \quad | \quad \sqrt{(\text{—}) \quad (\text{—}) \quad (\text{—})}$ (12)

This filter does not depend on the direction of magnetization and therefore remains useful where remanent magnetization is present and has effect on the RTP filter.

As a kind of RTP filter (Macleod et al., 1993), the analytical signal filter was applied to the total magnetic intensity grid of the intrusive dominated survey area to cater for the effect of remanent magnetization that the RTP filter could not take care of.

4.1.6.3 First Vertical Derivative

The first vertical derivative filter (1VD) which calculates the vertical gradient of the magnetic field was applied to the RTP grid. The 1VD filter accentuates high frequency relative to low frequency anomalies and for that matter remains useful in mapping textural variation in the data. The 1VD grid obtained was imaged and displayed as a greyscale intensity which enhanced the mapping of textural variation and geological structural trends.

4.2 Gravity Survey

Ground gravity survey of the study area was subsequently followed after the magnetic survey, between September and October 2015. All the resources used in this survey were also provided by Newmont Gold Ghana limited.

4.2.1 Gravity Survey Design

The demarcation used in the magnetic survey was kept for the gravity survey.
Gravity survey stations were set at 100m interval along the various traverse lines (Figure 4.1).

4.2.2 Instrumentation

Scintrix Auotograv CG-5 relative gravimeter was used for the gravity survey. It has an elastic molded quartz system which serves as the sensitive element. The known mass is balanced by a zero-length spring and a small electrostatic force. An automatic feed-back circuit generates an electrostatic force on the mass which brings it back to a null position. The measure of the relative gravity value is the feedback voltage.

High precision and accuracy of altitude in gravity survey requires the use of a differential GPS for elevation measurement.

Figure 4.3: Scintrex Autograv CG-5 gravimeter used for the survey

4.2.3 Field Data Acquisition

Acceleration due to gravity measurements were obtained for 626 gravity survey stations along the various traverse lines used in the magnetic survey at a station interval of 100m using Autograv Scintrix CG-5 gravimeter. At a gravity station, the gravimeter was gently placed on a tripod and leveled so that the instrument is suitable to measure accurately the gravity value at that station.

For each field acquisition day, gravity measurements were set off from the primary base station which has an absolute gravity value after which gravity stations along the traverse lines were occupied for gravity measurements and a return to the primary base station was made within 4 hours in order to monitor the effect of the instrumental drift. A station was set near the primary base station as a quality control measure for effective drift monitoring. Elevation coordinates of gravity stations were obtained using a differential GPS (Figure 4.4).

The gravimeter was handled gently to prevent oscillation of the spring. Again because the spring is highly affected by heat, an umbrella was used to shield the instrument during the survey. A field notebook was kept for recording the survey parameters.

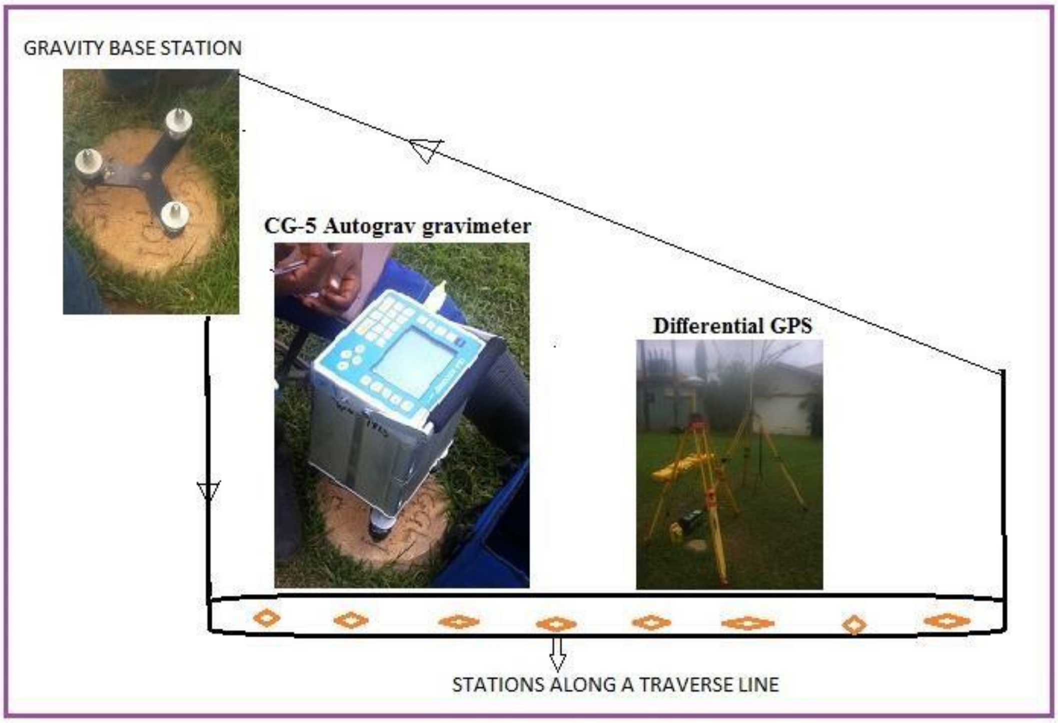

Figure 4.4: Schematic presentation of gravity data acquisition

4.2.4 Gravity Reductions

Gravity corrections were applied to the raw meter readings in order to obtain a gravity anomaly that was of geological interest. These corrections were to reduce the data to the mean sea level (geoid) and take out from the data the effects that which are not due to density variation. The *gravity* extension of the *oasis montaj* software was used to automatically apply the various corrections described below after the observed gravity readings were imported and synchronized.

4.2.4.1 Drift Correction

Instrumental drift caused by the creep in the quartz spring in the gravimeter was monitored with the primary base station that was set up. Drift correction of the data for each acquisition field day was applied automatically by referencing it to the primary base station where the survey began.

4.2.4.2 Latitude Correction

Latitude correction was performed to account for the change of observed gravity with change in latitude, which is due primarily to the rotation of the earth and the difference in earth radius between the poles and the equator. The latitude correction applied made use of the gravity formula 1967 (Mittermayer, 1969) given as; $g_ø = 9780318.5(1 +0$ $005278895 \sin^2ø +0.000023462 \sin^4ø)$ gu, (13)

where $g_ø$ is the predicted gravity value at particular latitude ø.

4.2.4.3 Free Air Correction

This correction made use of the variations in the elevation of the observed gravity stations which were moved to the geoid. This correction does not take into account the mass of the material existing between the gravity stations and the datum plane. A free air correction of 0.308596mGal/m was added to the observed gravity readings automatically by *oasis montaj*.

4.2.4.4 Bouguer Correction

The Bouguer correction (BC) was used to take care of the attraction of the materials existing between the gravity station and the geoid, which was disregarded during the free air correction. The Bouguer correction applied automatically with oasis montaj software assumed a mean earth density of 2.67 g/cc.

On land the Bouguer correction is subtracted and its formula is given as;

$$BC = 2\pi G\rho h = 0.4191\rho h \tag{14}$$

where G is Gravitational constant, ρ is density of rock mass and h is the orthometric height obtained from the elevation of the various stations acquired (Kearey et al. 2002).

4.2.4.5 Terrain Correction

This correction accounts for any surface irregularities in the vicinity of the various gravity stations, that is, hills rising above the gravity stations and valleys lying below it. The mass of a hill will cause gravity measurement to be deviated from the station (S1) and this will cause the acceleration due to gravity (F) to reduce and as such the correction has to be added. The same argument holds for the valley where deficiency in mass reduces the value of F and as such the correction has to be added (Figure 4.5).

The terrain correction applied made use of a digital elevation model (DEM) of the survey area to correct for the irregularities in the topographic relief in the vicinity.

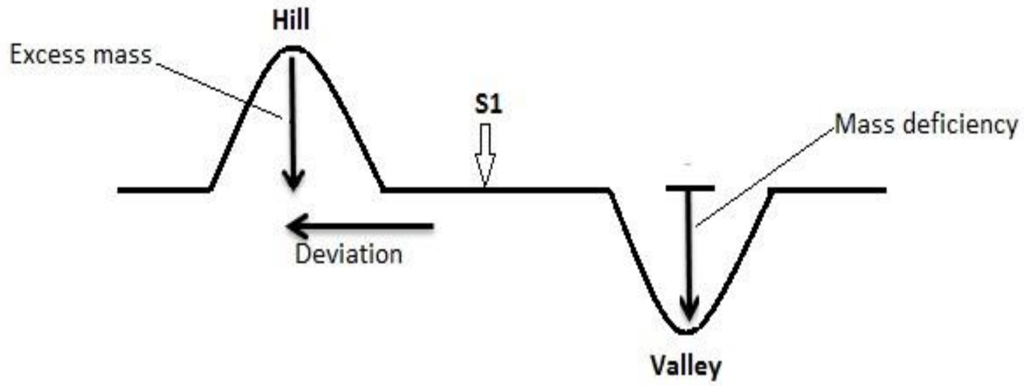

Figure 4.5: The terrain correction

4.2.5 Microlevelling

In order to filter a gridded dataset to remove non-geological effects which are caused by long wavelength anomalies, microlevelling technique is applied. These leveling defects were not removed during the regular data processing routines (Urquhart, 1988; Minty, 1991).

Microlevelling of the gravity data was achieved by using the MAGMAP extension of the *oasis montaj* software to apply a decorugation filter in the Fourier domain. The Butterworth high pass filter was placed at four times the spacing between traverse lines (400m) to produce an initial grid that compose of the leveling error. A filtered leveling channel was then created from the leveling error grid. Finally a microlevelled channel was acquired by deducting the filtered leveling channel from the complete Bouguer anomaly channel. The microlevelled channel was then gridded using the minimum curvature technique (Briggs, 1974) to obtain a microlevelled complete Bouguer anomaly grid.

4.2.6 Regional/Residual Separation

In order to emphasize residual anomaly which is of prime interest in mineral exploration, regional-residual separation technique was used to remove the regional constituent, which consist of deep seated bodies from the residual constituent, relating to shallow geological features.

A regional gravity grid of a 1km spacing regional gravity survey covering the southwestern portion of Ghana was subtracted from the microlevelled complete Bouguer anomaly grid using *grid-expression* module of the *oasis montaj* software to produce a final residual/local gravity anomaly.

CHAPTER 5 RESULTS AND DISCUSSIONS

Results from the processed and enhanced magnetic and gravity data are presented in this chapter in anomaly maps which show the contrast in magnetic susceptibility and density respectively. From the various results qualitative interpretation has been carried out in order to map out the various lithological units, structural features and zones relating to gold mineralization. These mapped features are correlated to areas where pockets of small scale mining operations (Galamsey) exist within the study area.

Geophysical anomaly map shows variations in a particular physical property of the underlying rocks due to some perturbations in its geometric distribution to produce a non-unique and indirect anomaly. Non-uniqueness of geophysical anomaly makes interpretation very difficult and therefore knowledge of the geology and mineralization targets is very essential for a comprehensive interpretation.

Geological evidence is the main test of geological meaning of a geophysical anomaly (Lyatsky et. al., 2005).

5.1 Magnetic Survey

Magnetic anomaly maps with different colours presented below show the contrast in the magnetic susceptibility of the subsurface geology. A Red/pink colour depicts areas with high magnetic susceptible rocks whereas blue colour relates to areas with low magnetic susceptible rocks. In mineral exploration, magnetic data is useful in mapping structures which serve as conduit for gold mineralized hydrothermal fluids and defining the various lithological units.

5.1.1 Total Magnetic Intensity Anomaly Map

Figure 5.1 is the total magnetic intensity anomaly map obtained after diurnal variation correction and removal of the IGRF model magnetic field from the observed magnetic intensity and gridded using the minimum curvature algorithm (Briggs, 1974).

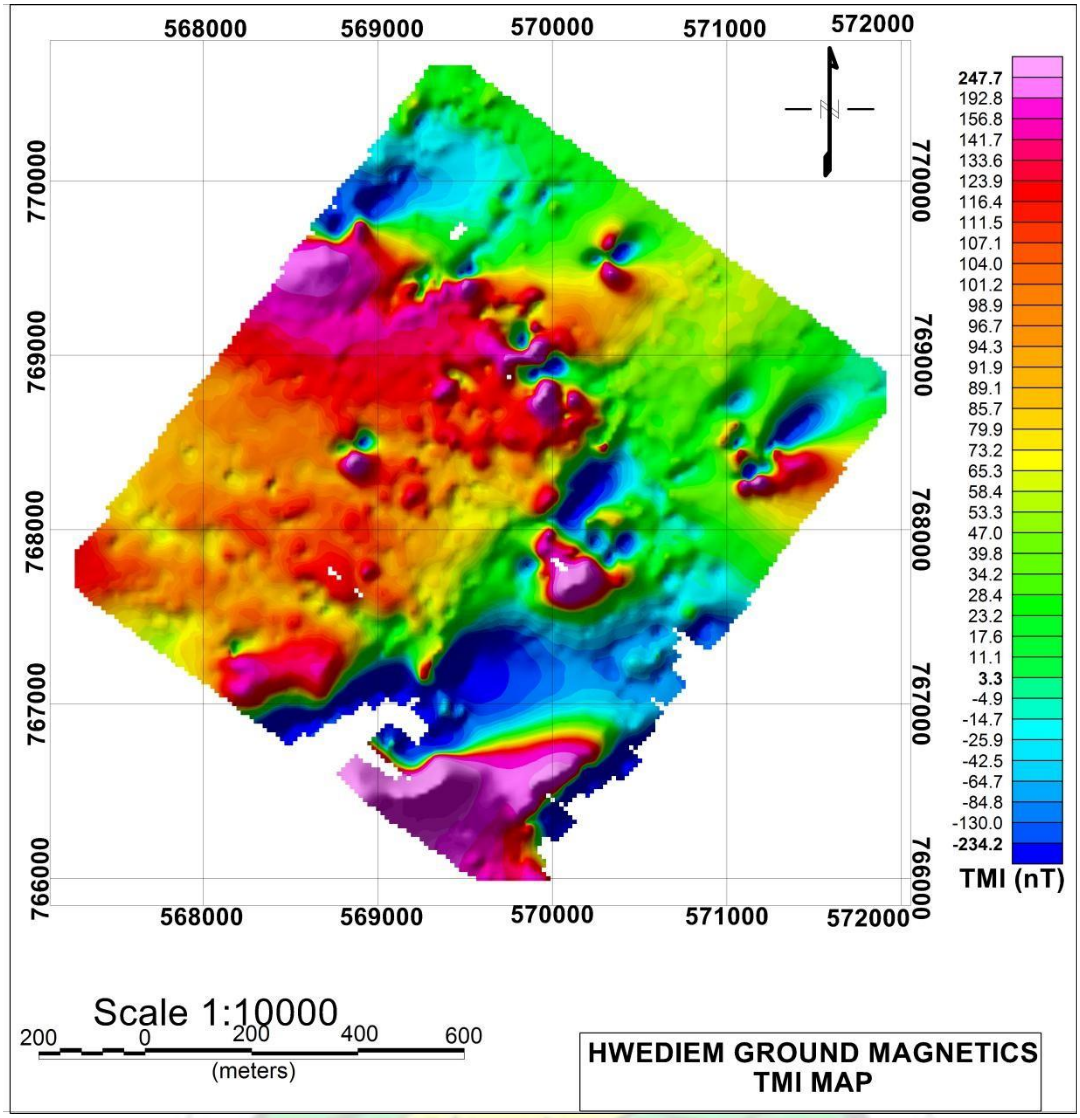

Figure 5.1: Total magnetic intensity map

The TMI anomaly map (Figure 5.1) has magnetic amplitude ranging from -234.2nT to 247.7nT. From the map, blue coloured zones are actually high magnetic zones which represent mafic intrusive units and the red to pink coloured zones are low magnetic anomaly areas which represent felsic intrusive units. This is because the study area located close to the equator where the magnetic field is inclined and anomalies asymmetric about its causative body makes interpretation complex (Milligun and Gunn, 1997). This effect is taken care of by applying the reduction to the pole filter to the total magnetic intensity data.

5.1.2 Reduction to the Pole Map

The RTP filter used on the TMI was able to remove the effect of asymmetric nature of anomalies that was due to inclined induced magnetic field by converting it to the magnetic pole where the magnetic field is vertical and anomalies are symmetric.

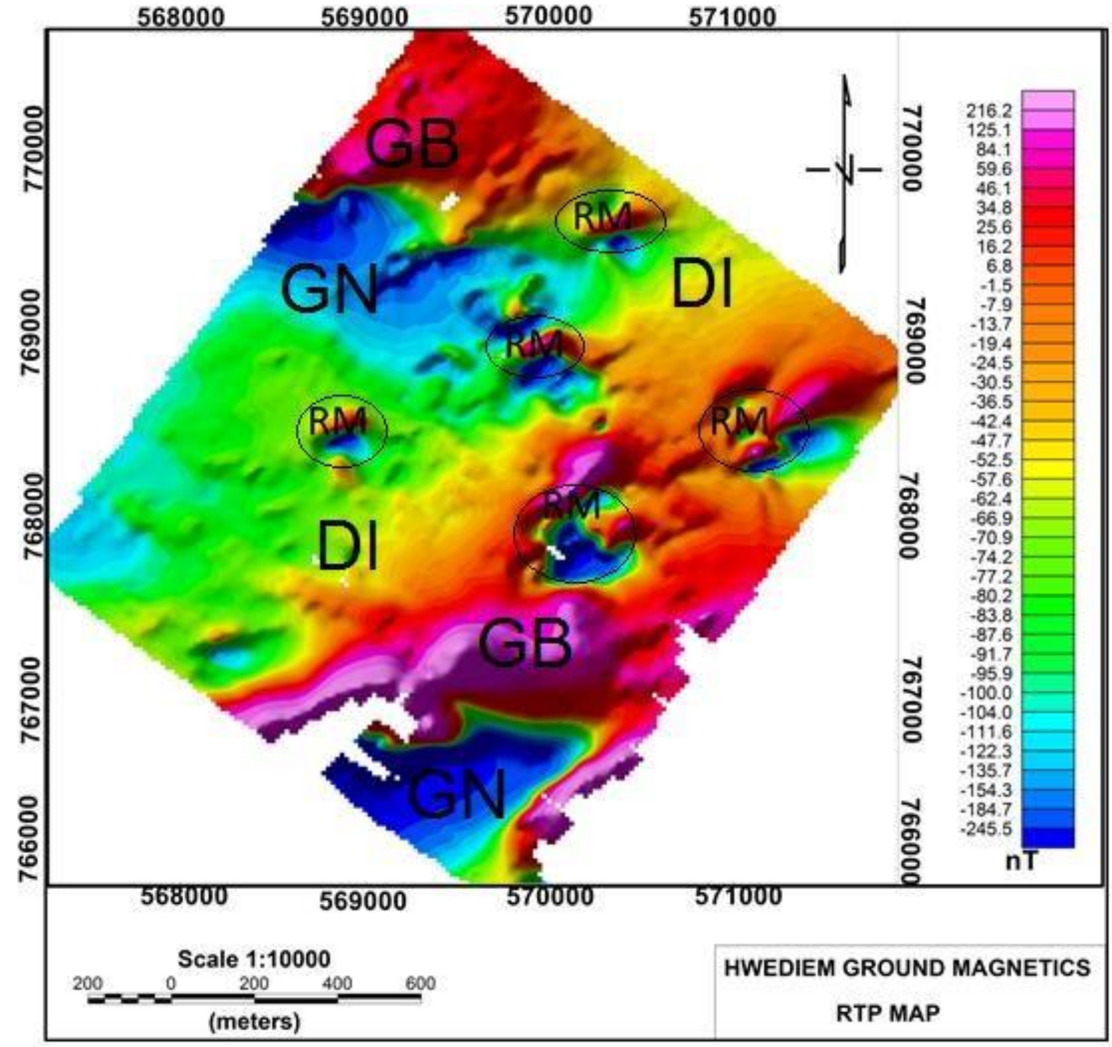

Figure 5.2: Reduction to the pole map

Figure 5.2 is the RTP anomaly map shown above in which magnetic signatures are simplified thereby having high susceptible geology to have a high magnetic intensity (red to pink) and low magnetic susceptible geological formations to have a low magnetic intensity anomaly (green to blue) unlike the TMI map (Figure 5.1). From the RTP map, high magnetic anomalous zones (GB) are related to a mafic intrusive unit containing more magnetic minerals. A moderate to high magnetic anomalous zones (DI) and relatively low magnetic anomalous zones (GN) are also related to the paleoproterozoic Birimian belt type (Dixcove) granitoids.

The RTP is inhibited by the presence of remanence because it assumes all magnetization is due to induced magnetization (Milligun and Gunn, 1997). From the RTP map, the effect of remanence (RM) is well pronounced due to the reversal of the magnetic field.

5.1.3 Analytical Signal Map

At low magnetic latitudes like Ghana where the RTP filter has trouble, the analytical signal filter becomes very useful (Milligun and Gunn, 1997). The analytical signal filter which is independent of the direction of magnetization is used as a type of RTP filter to remove the effect of remanence by maximizing the edges of magnetized bodies (MacLeod et al., 1993).

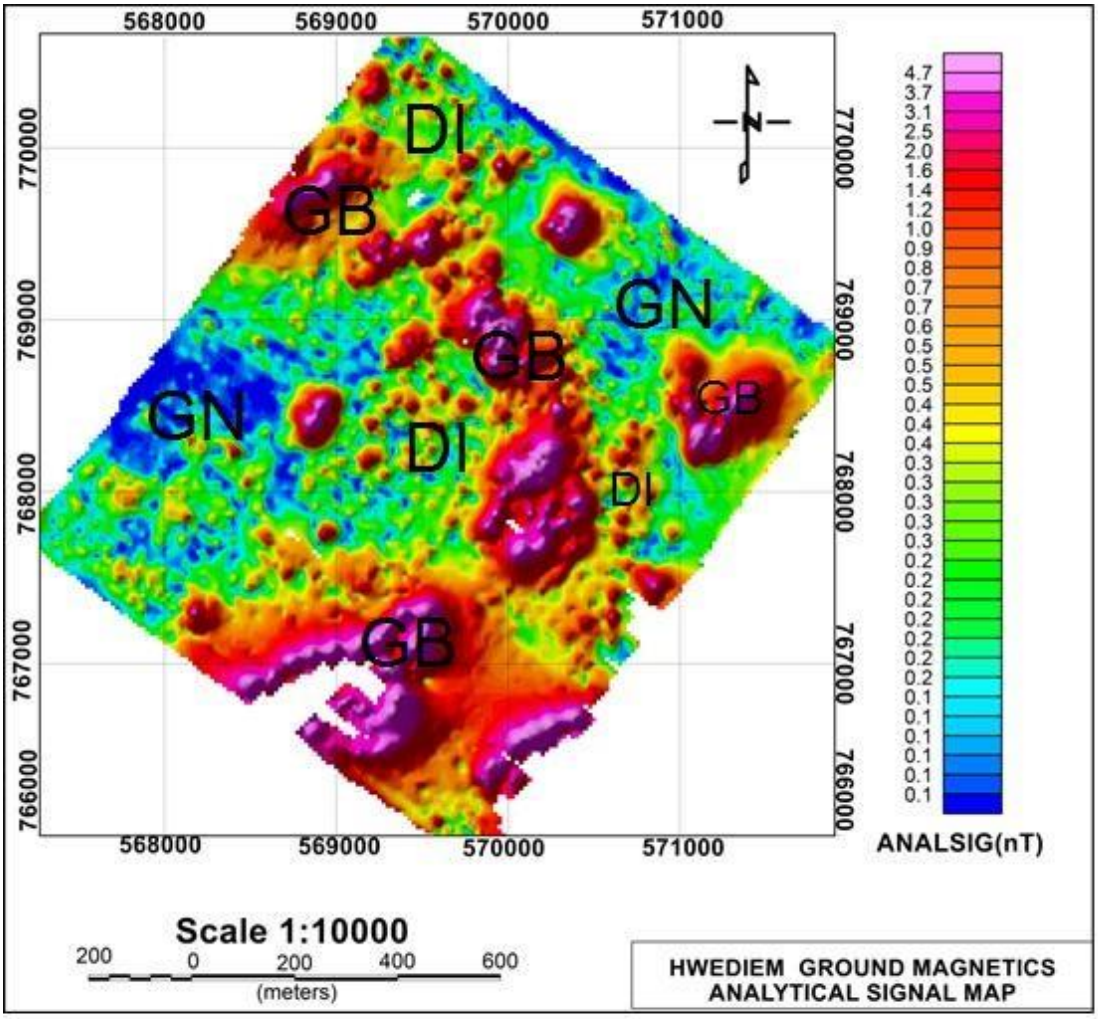

Figure 5.3: Analytical signal map

Figure 5.3 is the analytical signal map which shows well-defined and positioned magnetic signatures as compared to the TMI and RTP maps. The effect of remanence (RM) in the RTP map (Figure 5.2) has been corrected by putting a high over the top of any magnetic anomaly (high or low) regardless of the direction of magnetization. Three magnetic signatures have been mapped from the analytical signal map. High magnetic amplitude (GB) correlates to a mafic intrusive unit. Intermediate magnetic amplitude (DI) is correlated to the Birimian belt type granitoids. Low magnetic signature (GN) which is bounded by the intermediate magnetic signature is also correlated to the Birimian belt type granitoids.

5.1.4 First Vertical Derivative Map

Figure 5.4 is the first vertical derivative (1VD) map of the RTP which is displayed in grey colour to enhance interpretation. The 1VD filter has been useful in sharpening short wavelength magnetic anomalies at the expense of high wavelength magnetic anomalies making it useful in elevating textural variation in the data.

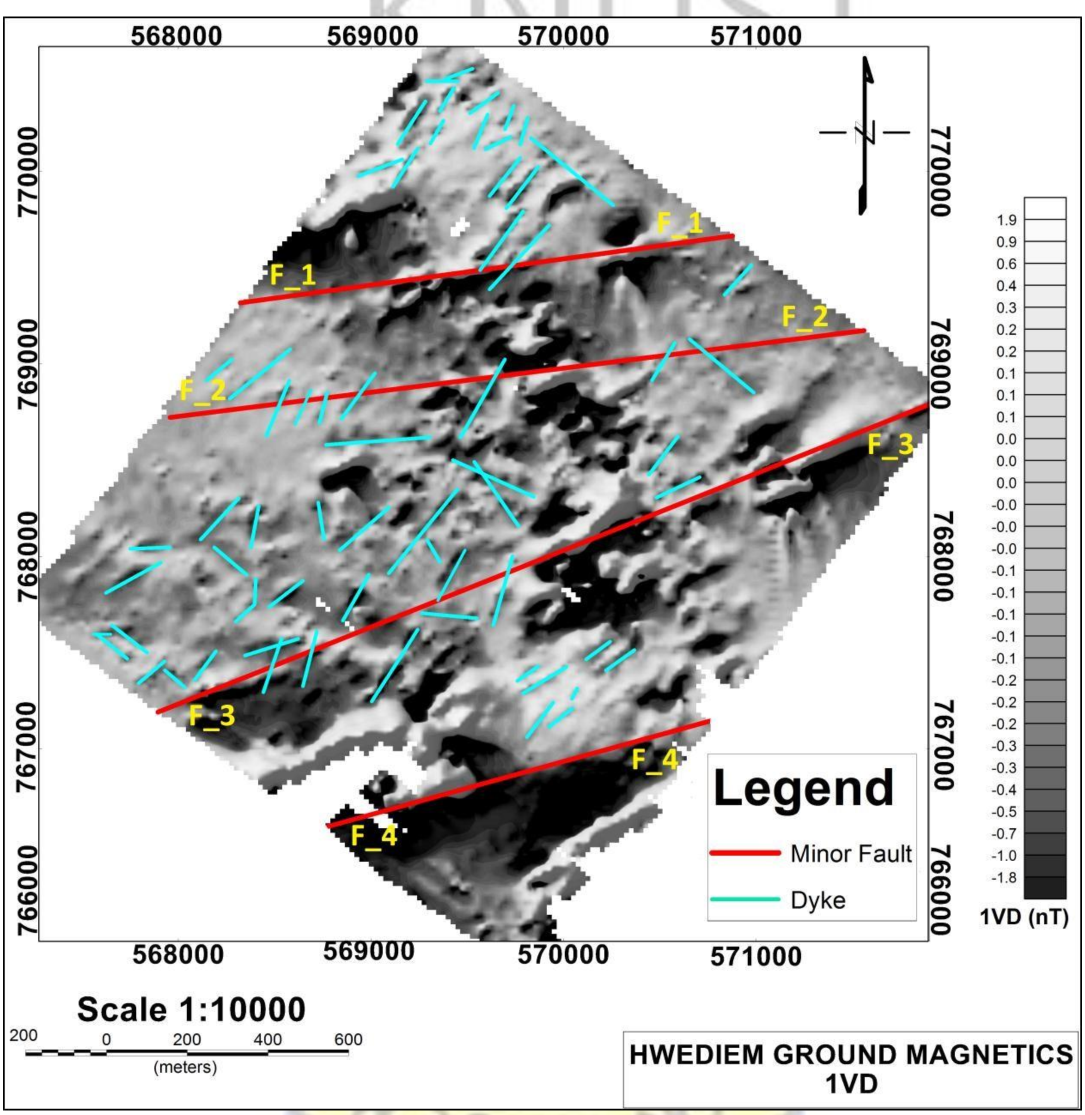

Figure 5.4: First vertical derivative map in greyscale

The study area is in an intrusive dominated lithology which falls off the main structural trend (Kenyasi shear zone) in the area (Ahafo Mineral Resource/Reserve

Report, 2006). Four main NE/SW minor linear structures (F_1--F_1, F_2--F_2, F_3—F_3, F_4--F_4) marked with red lines are interpreted to represent minor faults.

Crosscutting the minor faults are extensive dykes that are marked with green lines.

5.2 Results from Gravity Survey

Results from gravity survey which depends on the lateral variation in subsurface rock density are presented. Residual gravity anomalies are presented as maps (images) with high gravity values (red-pink) relating to a more denser rocks and low gravity values (blue) relating to less dense rocks.

5.2.1 Complete Bouguer Anomaly

Figure 5.5 is the complete bouguer anomaly map which is obtained after the necessary reductions are applied to isolate the variations due to density of the subsurface rock. The complete Bouguer anomaly consists of regional and residual anomalies superimposed over each other. Three major gravity features are mapped in the area which is generally NE/SW gravity gradient with a decreasing regional tendency from east to west. The southern and eastern portions are characterized by high gravity gradient (B1) which is associated with a dense mafic intrusive unit. A low gravity gradient characterizes the western part (B3) representing a low dense material. A moderate gravity gradient (B2) is located between the high and low gravity gradients. The low to moderate gravity gradients are believed to be associated with the Birimian belt type granitoids.

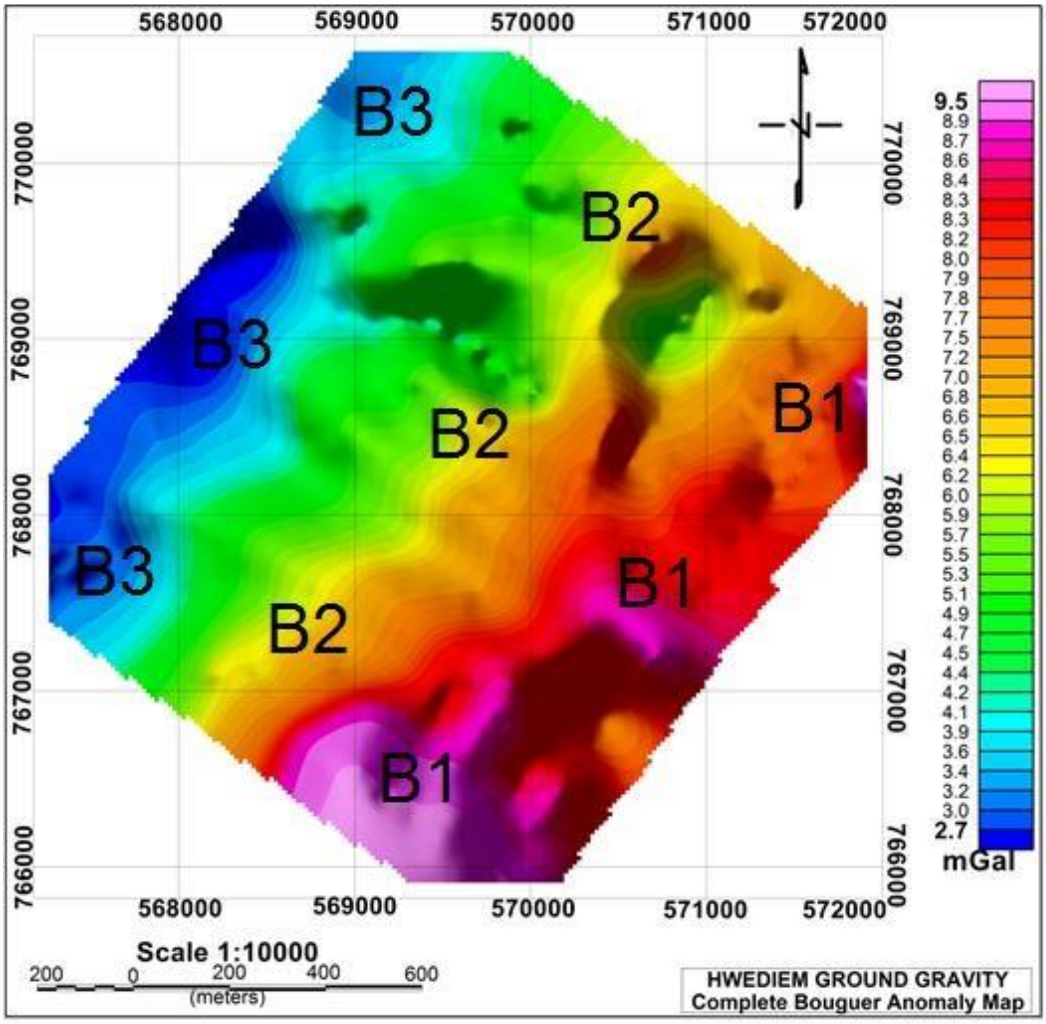

Figure 5.5: Complete Bouguer anomaly map

5.2.2 Residual Gravity Anomaly Map

Figure 5.6 is the Residual gravity anomaly map obtained after the regional gravity constituent was taken out from the complete Bouguer anomaly. Anomalies with long wavelength anomalies have been checked thereby amplifying anomalies with short wavelength. Figure 5.6 shows that shallow seated anomalies have been outlined explicitly and sharpened as against the CBA (Figure 5.5). From the map three main gravity anomaly features have been mapped. Near surface excess mass (GB in Figure

5.6) occurs at portions of the southern, eastern and northern part of the area. This gravity signature is correlated to a mafic intrusive unit referred as Gabbro.

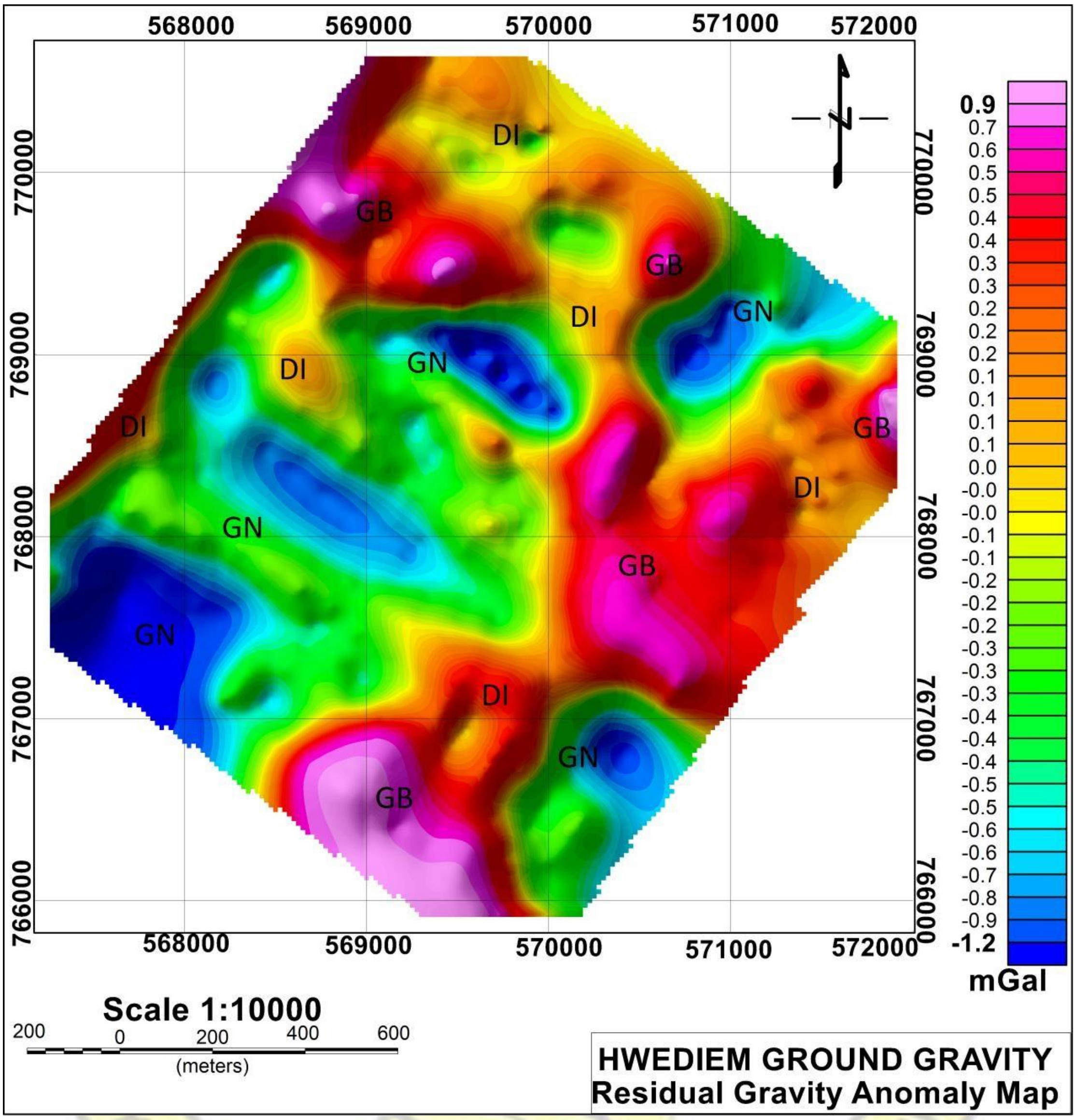

Figure 5.6: Residual gravity anomaly map

Intermediate gravity anomaly (DI in figure 5.6) is found at portions of the southern, eastern, northern, western and central part of the area. This gravity anomaly is correlated to the Birimian belt type (Dixcove) granitoids and is believed to be dioritic. A low gravity anomalous zone (GN in figure 5.6) is also related to the

Birimian belt type granitoids referred to as granodiorite.

5.3 Geological Map from Integrated Magnetic and Gravity Data

Results from gravity and magnetic datasets, corroborated by regional scale geology of the area have been used to generate a geological map for the survey area as presented in Figure 5.7. The TMI map, reduced to the pole map, analytical signal and the residual gravity anomaly map have been useful in mapping out the various lithological units. The first vertical derivative in conjunction with the residual gravity anomaly maps has also been helpful in defining the structural features in the area. From Figure 5.7, three main lithological have been defined.

A low magnetic susceptibility and density signatures (yellow areas) correlated to the paleoproterozoic Birimian belt type (Dixcove) granitoids referred to as granodiorite. This is located in the southwestern, northeastern and central parts of the area. Intermediate gravity and magnetic signatures (pink zones) are also associated to the Dixcove granitoid believed to be diorite. Intruding into the belt type dioritic lithology is a high magnetic and gravity anomaly (brown zones) correlated to a mafic intrusive unit inferred as gabbro.

NE/SW trending minor faults have been mapped which run though the various lithologies and is believed to be associated with the Eburnean orogenic event. Dykes are generally concentrated in the areas of the Dixcove granitoids which crosscut the minor faults.

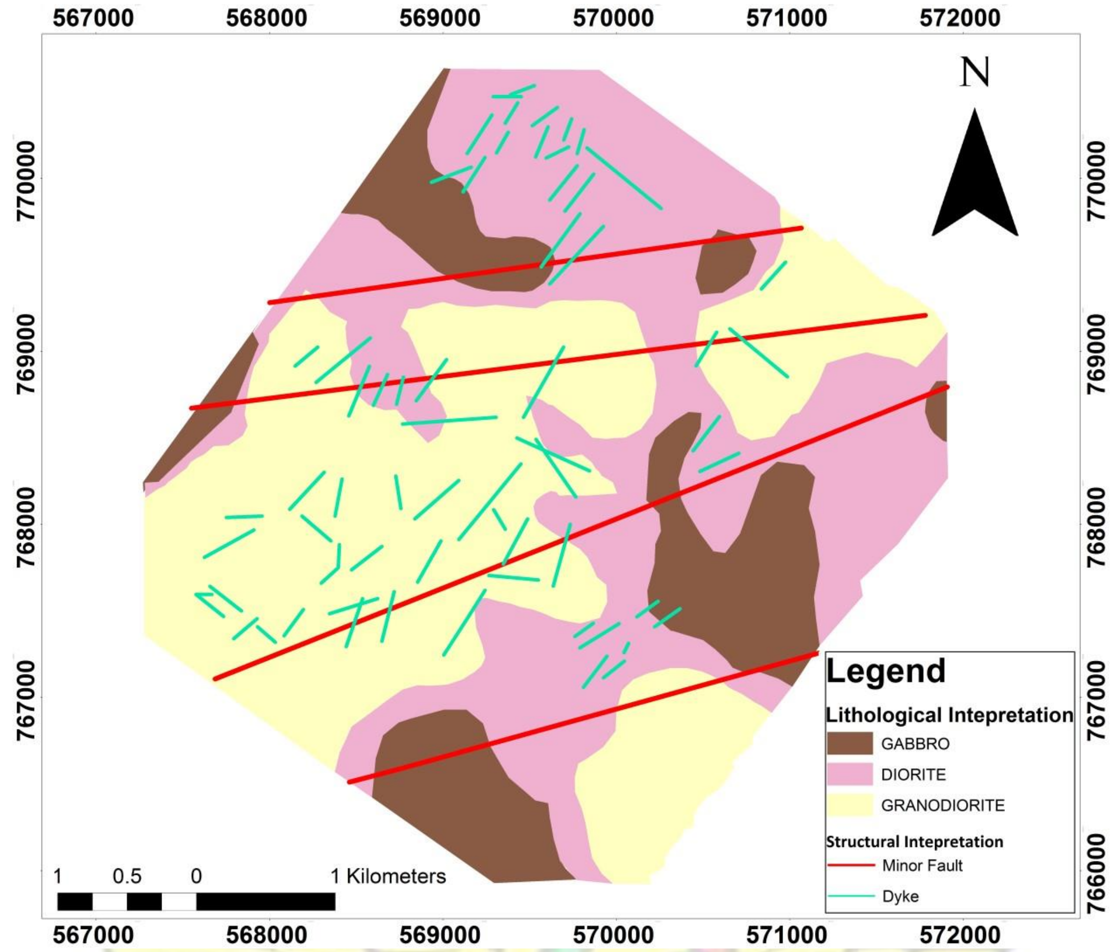

Figure 5.7: Proposed geological map of the study area

5.4 Relating Galamsey Sites to Proposed Geology

The sites of small gold mining operations (Galamsey) in the study area have been located and related to the proposed geology (Figure 5.8). From Figure 5.8 the three main Galamsey sites referred to as *Target 1, 2* and *3* are described below.

Target 1 is situated at the western section of the survey area and falls within the granodioritic unit and extends into the dioritic unit. It also falls on a NE/SW minor fault associated with series of extensive dykes which crosscut the minor fault.

Target 2 is the largest among the three mapped Galamsey sites in the area. It is located mainly within the granodioritic unit in the southwestern section of the area that trends in the NE/SW direction. *Target 2* falls on a NE/SW minor fault and it is also associated with crosscutting dykes.

Target 3 is the smallest among the three mapped sites situated at the southeastern section of the survey area. It also lies on a NE/SW minor fault and falls within two main lithological units; diorite and granodiorite.

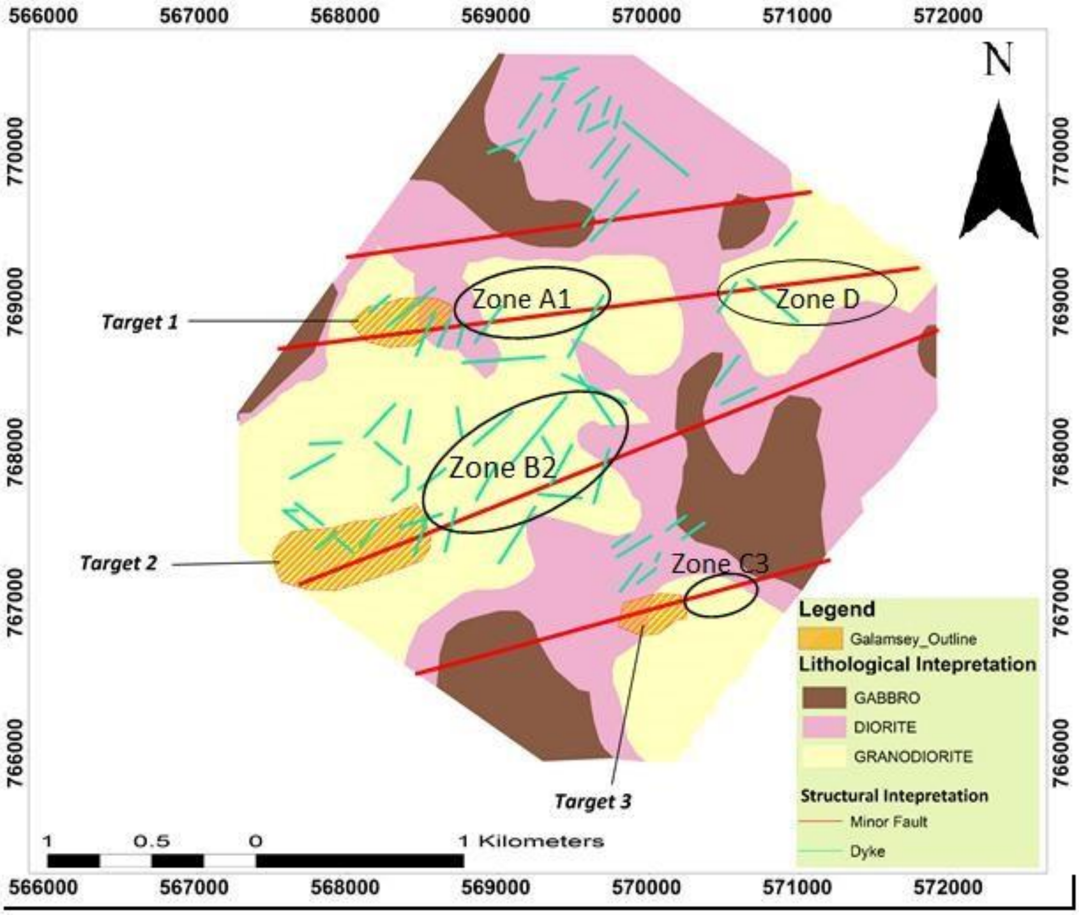

Figure 5.8: Galamsey sites and potential gold mineralization zones from the proposed geology

5.5 Proposed Gold Mineralization Zones

The mapped lithology, structural trends and Galamsey sites (*Targets*) have been used in delineating potential gold mineralized areas in the study area. One interesting observation is that all the Gold targets lie on a minor fault and are related to the granodiorite and diorite units (Figure 5.8). Gold mineralization is believed to be associated with the minor faults which could have functioned as a conduit for mineralized hydrothermal fluids related to the Eburnean orogenic event.

Four potential gold mineralized zones are delineated in the study area (Figure 5.8). Zones A1 and C3 relate to *Target 1* and *Target 3* in the western and southeastern part respectively. These zones fall on granodioritic to dioritic belt type granitoids and sit on minor faults. Zone B2 is the extensive delineated zone that relates to *Target* 2 falling mainly in a granodioritic unit though it extends a little into the dioritic unit in the central part of the area and it is associated with crosscutting dykes. Zone D does not relate to any *Target* but falls on the same minor fault as zone A1 at the northeastern corner in a granodioritic unit. It is marked as a favorable zone because of its similarities with the other zones.

CHAPTER 6 CONCLUSIONS AND RECOMMENDATIONS

6.1 Conclusions

Ground gravity and magnetic survey have been used to map out the lithological units at the Hwediem concession. The residual gravity anomaly and the magnetic filters TMI, RTP and analytical signal have been helpful in mapping out the various lithological units. High magnetic anomaly signature in the analytical signal image was used in delineating the mafic intrusive units correlated to gabbro. The residual gravity anomaly image also sharpened and defined the mafic intrusive unit as high gravity values. Low and intermediate gravity zones from the residual gravity anomaly map representing low and intermediate dense rock correlated to granodioric and dioritic belt type (Dixcove) Birimian granitoids respectively. The RTP and the analytical signal maps also gave a similar response in the western and eastern part.

The geological structural trend of the area was mapped mainly using the magnetic data. The 1VD map helped to define the NE/SW minor faults and the crosscutting dykes largely concentrated in the Birimian belt type granitoids.

Small scale gold mining operational sites (Galamsey) referred to as ‗Targets' were mapped and related to the mapped geology of the area. *Target 1* and *3* were located within granodioritic to dioritic units which sit on minor faults. Target 2 was located in granodioritic unit and also sits on minor fault associated with crosscutting dykes.

With the mapped lithology, structural geology and the Galamsey sites (*Targets*), four Zones of potential gold mineralization have been delineated. Zone A1 and C3 relate to target 1 and 3 respectively and also fall on minor faults associated with crosscutting dykes. Zone B2 is the extensive delineated zone which also falls on a minor fault in a granodioritic unit extending a little into a dioritic unit. Zone D is not related to any Galemsey site (*Target*) but similar to the other delineated zones.

6.2 Recommendations

A 3D inversion of the gravity and magnetic data should be undertaken to ascertain the density and magnetic susceptibility distribution respectively with depth and shape. This will increase the accuracy and confidence in placing test drills.

Again a geochemical survey is should be undertaken at the proposed potential zones of gold mineralization to give a detailed trend of mineralization. Further research such as geochemistry should be conducted at areas along the minor fault at the northern part of the area, F_1--F_1 (Fig 5.4) which does not relate to any Target. This will be helpful because this minor fault could have also served as a conduit for hydrothermal fluids which might have been mineralized.

It is also recommended that this study should be replicated in areas with similar geological setting where small scale mines (Galamsey) exist with their controlling structures unknown.

References

Ahafo Mineral Resource and Ore Reserve Report (2006). Newmont Ghana Gold Limited, Ahafo Project

Airo, M.-L., and Mertanen, S. (2008). Magnetic Signatures Related to Orogenic Gold Mineralization, Central Lapland Greenstone Belt, Finland. *Journal of Applied Geophysics*, *64*(1-2), 14–24. http://doi.org/10.1016/j.jappgeo.2007.10.003

Baranov, V. and Naudy, H. (1964). Numerical Calculation of the Formula of Reduction to the Magnetic Pole. Geophysics, 29, 67–79

Bishop, J. R. and Emerson, D. W. (1999), Geophysical properties of zinc-bearing deposits. Australian Journal of Earth Sciences, 46: 311–328. doi: 10.1046/j. 1440-0952.1999.00706.x

Briggs I.C. (*1974). Machine Contouring Using Minimum Curvature. Geophysics, 39, 39–48.*

Chen, G., Liu, T., Sun, J., Cheng, Q., Sahoo, B., Zhang, Z., and Zhang, H. (2015). Gravity Method for Investigating the Geological Structures Associated with W-Sn Polymetallic Deposits in the Nanling Range, China. *Journal Of Applied Geophysics*. Http://Doi.Org/10.1016/J.Jappgeo.2015.06.001

Griffis, R., Barning, K., Agezo, F., and Akosah, F. (2002). *Gold Deposits of Ghana. Minerals commission.*

Hinson, G., Menyeh, A., and Wemegah, D. D. (2015). Qualitative Interpretation of Aerogravity and Aeromagnetic Survey Data over The South Western Part of the Volta River Basin of Ghana. International Journal of Scientific and Technology Research, 4, 23-30.

Junner, N. (1935). Gold in gold coast. Accra, Ghana: Gold Coast Geological survey Memoir, 4, 67p.

Kearey, P., Brooks, M., and Hill, I. (2002). *An Introduction to Geophysical Exploration* (Third edit). Blackwell Science Ltd.

Kesse, G.O. (1985). *The Mineral and Rock Resources of Ghana*. A.A. Balkema/Rotterdam/Boston.

Leube, A., Hirdes, W., Mauer, R., Kesse, G. O., Rohstoffe, G., and G, D.-H. F. R. (1990). The Early Proterozoic Birimian Supergroup of Ghana and Some Aspects of its Associated Gold Mineralization. *Precambrian Research*, *46*, 139–165.

Lyatsky, H.V., Pana, D.I., and Grobe, M. (2005). Basement Structure in Central and Southern Alberta: Insights from Gravity and Magnetic Maps, EUB/AGS Special Report, Vol. 72, 2005, pp. 1-83.

MacLeod, I.N., Jones K., and Dai,T.F. (1993). 3-D Analytic Signal in the Interpretation of Total Magnetic Field Data at Low Magnetic Latitudes. Exploration Geophysics, 24(4), 679–688

Milligan, P. R. and Gunn, P. J. (1997). Enhancement and presentation of airborne geophysical data. AGSO Journal of Australian Geology and Geophysics, 17(2):64–774.

Minty, B.R.S. (1991). Simple microlevelling for aeromagnetic data. Exploration Geophysics, 22, 591-592

Mittermayer, E. (1969). Numeriacla Formulas for the Geodetic Reference System 1967. Bolletino di Geofisca Teorica ed Applicata, 11, 96-107.

Nabighian, M.N. (1972). The analytical signal of two-dimensional magnetic bodies with polygonal cross-section: its properties and use for automated anomaly interpretation. *Geophysics*, 37(3): 507-517.

Nabighian, M. N., Grauch, V. . J. S., Hansen, T. M., Lafehr, T. R., and Peirce, J. W. (2005). 75th Anniversary The development of the magnetic method in exploration. *Geophysics*, *70*(6).

Oberthor, T., Schmidt Mumm, A., Vetter, U., Simon, K., and Amanor, J. A. (1996). Genetic Constraints of the Stable Isotope Geochemistry. Economic Geology, 91, 289–301.

Parasnis, D. S. (1979). *Principles of Applied Geophysics* (Third Edition). Chapman and Hall Ltd.

Reynolds, J. M. (1997). *An Introduction to applied and Environmental Geophysics*. John Wiley & Sons Ltd.

Roest, W.R., Verhoef, J. and Pilkington, M. (1992). Magnetic Interpretation using the 3-D analytical signal. Geophysics, 57:116-125.

Sestini, G. (1973). ―Sedimentology of a Paleoplacer; The Gold Bearing of Tarkwaian of Ghana: Ores in sediments‖, *International Union of Geological Sciences*, Series A, No. 3, pp. 269-278.

Sharma, P. V. (1986). Geophysical Methods in Geology. New York, Elsevier Science Puplishing Co., Inc.

Sharma, P. V. (1987). Magnetic Method Applied to Mineral Exploration. Ore geology reviews 2(4), 323–357.

Taylor, P. N., Moorbath, S., Leube, A., and Hirdes, W. (1992). Early Proterozoic Crustal evolution in Birimian of Ghana: constraints from geochronology and isotope geochemistry. Precambrian Research, *56*, 97–111.

Telford, W. ., Geldart, L. ., and Sheriff, R. (1990). *Applied Geophysics* (second edi).

Urquhart, T., (1988). Decorrugation Of Enhanced Magnetic Field Maps: Expanded Abstracts and Biographies, Society of Exploration Geophysicists 58th Annual Meeting, 371-372.

Wemegah, D.D., Preko, K., Noye, R.M., Boadi, B., Menyeh, A., Danuor, S.K. and Amenyoh, T. (2015). Geophysical Interpretation of Possible Gold Mineralization Zones in Kyerano, South-Western Ghana Using Aeromagneticand Radiometric Datasets. *Journal of Geoscience and Environment Protection*, **3**, 67-82. Cambridge Unversity Press.

Yao, Y., and Robb, L. . (2000). Gold mineralization in Palaeoproterozoic granitoids at Obuasi , Ashanti region , Ghana : Ore geology , geochemistry and fluid characteristics, *103*, 255–278.